



Design and synthesis of novel DFG-out RAF/vascular endothelial growth factor receptor 2 (VEGFR2) inhibitors: 3. Evaluation of 5-amino-linked thiazolo[5,4-*d*]pyrimidine and thiazolo[5,4-*b*]pyridine derivatives

Masaaki Hirose^{a,*}, Masanori Okaniwa^{a,*}, Tohru Miyazaki^a, Takashi Imada^a, Tomohiro Ohashi^a, Yuta Tanaka^a, Takeo Arita^a, Masato Yabuki^a, Tomohiro Kawamoto^a, Shunichirou Tsutsumi^b, Akihiko Sumita^b, Terufumi Takagi^a, Bi-Ching Sang^c, Jason Yano^c, Kathleen Aertgeerts^c, Sei Yoshida^a, Tomoyasu Ishikawa^{a,*}

^a Pharmaceutical Research Division, Takeda Pharmaceutical Company Limited: 26-1, Muraoka-Higashi 2-chome, Fujisawa, Kanagawa 251-8555, Japan

^b CMC Center, Takeda Pharmaceutical Company Limited: 17-85, Jusohonmachi 2-chome, Yodogawa-ku, Osaka 532-8686, Japan

^c Structural Biology, Takeda California Inc., 10410 Science Center Drive, San Diego, CA 92121, USA

ARTICLE INFO

Article history:

Received 13 June 2012

Revised 9 July 2012

Accepted 11 July 2012

Available online 23 July 2012

Keywords:

RAF

VEGFR2

Solubility

Oral absorption

Antitumor efficacy

ABSTRACT

Our aim was to discover RAF/vascular endothelial growth factor receptor 2 (VEGFR2) inhibitors that possess strong activity and sufficient oral absorption, and thus, we selected a 5-amino-linked thiazolo[5,4-*d*]pyrimidine derivative as the lead compound because of its potential kinase inhibitory activities and its desired solubility. The novel tertiary 1-cyano-1-methylethoxy substituent was designed to occupy the hydrophobic region of 'back pocket' of BRAF on the basis of the X-ray co-crystal structure data of BRAF. In addition, we found that N-methylation of the amine linker could control the twisted molecular conformation leading to improved solubility. These approaches produced *N*-methyl thiazolo[5,4-*b*]pyridine-5-amine derivative **5**. To maximize the *in vivo* efficacy, we attempted salt formation of **5**. Our result indicated that the besylate monohydrate salt form (**5c**) showed significant improvement of both solubility and oral absorption. Owing to the improved physicochemical properties, compound **5c** demonstrated regressive antitumor efficacy in a HT-29 xenograft model.

© 2012 Elsevier Ltd. All rights reserved.

1. Introduction

Members belonging to the RAF family are important molecules involved in signal transduction of the mitogen-activated protein kinase (MAPK) pathway associated with the cellular proliferation, differentiation, and survival.¹ Oncogenic mutations of *BRAF* are frequently observed in many cancers and cause abnormal proliferation without any control by receptor tyrosine kinases (RTKs).² In addition, the signaling between the vascular endothelial growth factor (VEGF) and VEGF receptor 2 (VEGFR2) plays a significant role in the process of progression of solid tumors.³ Many solid tumors require sufficient amount of nourishment for their progression

Abbreviations: ¹H NMR, proton nuclear magnetic resonance; AUC, area under the blood concentration/time curve; ERK, extracellular signal-regulated kinase; HUVEC, human umbilical vein endothelial cells; MEK, mitogen-activated protein kinase; PK, pharmacokinetic; VEGFR2, vascular endothelial growth factor receptor 2.

* Corresponding authors. Tel.: +81 466 32 1029 (M.H.), +81 466 32 1158 (M.O.), +81 466 32 1155 (T.I.).

E-mail addresses: masaaki.hirose@takeda.com (M. Hirose), masanori.okaniwa@takeda.com (M. Okaniwa), tomoyasu.ishikawa@takeda.com (T. Ishikawa).

and therefore they construct blood vessels by producing VEGF, which stimulates adjacent VEGFR2. Thus, BRAF and VEGFR2 are independently associated with exacerbation of solid tumors. Based on the evidence, inhibitors of BRAF and VEGFR2 could be effective therapeutic agents for cancer treatment.⁴

During drug discovery, the efficacy of a small molecule is generally determined not only by its binding affinity to target proteins but also by its physicochemical properties. Despite the excellent *in vitro* potency of the molecule, physicochemical properties such as low solubility and low metabolic stability have a negative impact on the pharmacokinetic (PK) profiles and the *in vivo* efficacy of the molecule. Therefore, improvement of the physicochemical properties of the drug candidates by optimization of highly potent lead compounds is a necessary process for drug discovery.

Previously, we reported the design, synthesis, and characterization of 2-chloro-3-(1-cyanocyclopropyl)-*N*-[5-({2-[(cyclopropylcarbonyl)amino][1,3]thiazolo[5,4-*b*]pyridin-5-yl}oxy)-2-fluorophenyl]benzamide **1** as a highly potent RAF/VEGFR2 inhibitor (IC₅₀ values: BRAF, 7.0 nM and VEGFR2, 2.2 nM; Fig. 1).⁵ Although this compound showed excellent *in vitro* cellular activity (pMEK

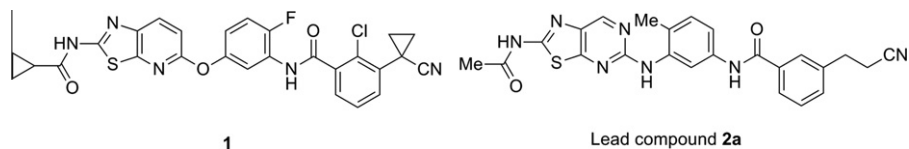


Figure 1. Chemical structures of the previous RAF/VEGFR2 inhibitor **1** and lead compound **2a**.

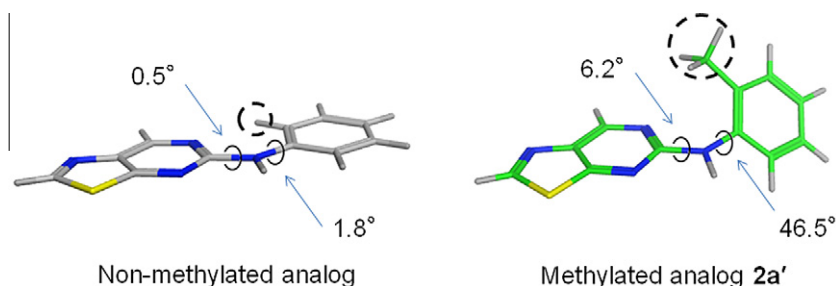


Figure 2. Stable conformations calculated for simplified methylated analog **2a'** (green) and non-methylated compound (gray). Simplified analog of **2a** shows twisted conformation between anilino benzene and [1,3]thiazolo[5,4-*d*]pyrimidine with increased dihedral angles of 46.5° and 6.2° compared to the almost planar conformation of the non-methylated compound.

($IC_{50} = 25$ nM), the oral PK profiles were poor and *in vivo* efficacy was weak because of its low thermodynamic solubility (3.6 $\mu\text{g}/\text{mL}$) without assistance of formulation technology⁵ or prodrug approach.⁶

Setting back to other potential chemotypes possessing sufficient drug-like properties could be one of the solutions for drug discovery. In particular, if X-ray co-crystal structure information of the target protein is available, chemical modification starting from other chemotypes could be strategic and productive. Therefore, we explored an alternative chemotype to discover RAF/VEGFR2 inhibitors that possess strong activity as well as sufficient solubility and oral PK profiles.

We found that 5-amino-linked [1,3]thiazolo[5,4-*d*]pyrimidine derivative **2a** possesses sufficient solubility (34 $\mu\text{g}/\text{mL}$) (Fig. 1). We assumed that good solubility of **2a** may be because of an increase in the dihedral angle⁷ by introducing the methyl group at the *ortho* position of the anilino benzene moiety (Fig. 2). Computational analysis for scanning stable conformations indicated that the methylated analog **2a'**, simplified compound of **2a** for this calculation,

shows twisted conformation between the anilino benzene and [1,3]thiazolo[5,4-*d*]pyrimidine scaffold with increased dihedral angles of 46.5° and 6.2° as a stable conformation compared to the almost planar conformation of the corresponding non-methylated compound. Some studies reported that a twisted molecular conformation contributes to augmenting the crystal packing energy, thus improving the dissolution rate as well as solubility.^{7–10} Thus, we hypothesized that twisted conformation of 5-amino-linked moiety between the aniline benzene moiety and the bicyclic scaffold may have an impact on improving solubility in aqueous media. Furthermore, compound **2a** showed potential inhibitory activity against both BRAF and VEGFR2 (IC_{50} values: BRAF, 51 nM and VEGFR2, 410 nM) as a lead compound. Therefore, we initiated a lead optimization of 5-amino-linked chemotype (**2a**) using a structure-guided drug design based on co-crystal structural information of BRAF protein.

We reported that the *in vitro* cellular pMEK inhibitory activity of our BRAF inhibitors was affected by the bulkiness of the substituent at the R^{3b} position of ring C (Fig. 3).⁵ According to co-crystal

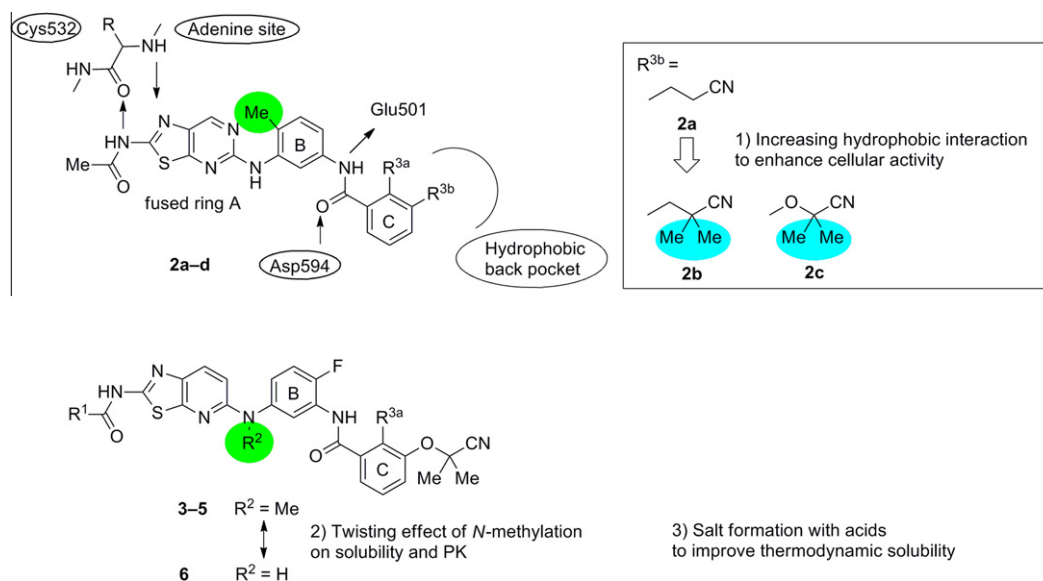


Figure 3. Design concept of DFG-out type RAF/VEGFR2 inhibitors.

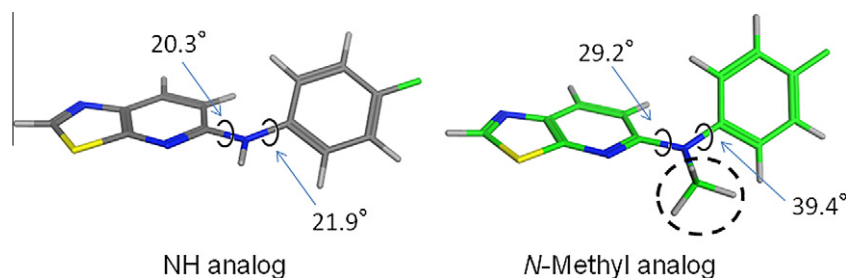


Figure 4. Stable conformations calculated for simplified *N*-methyl analog (green) and NH analog (gray).

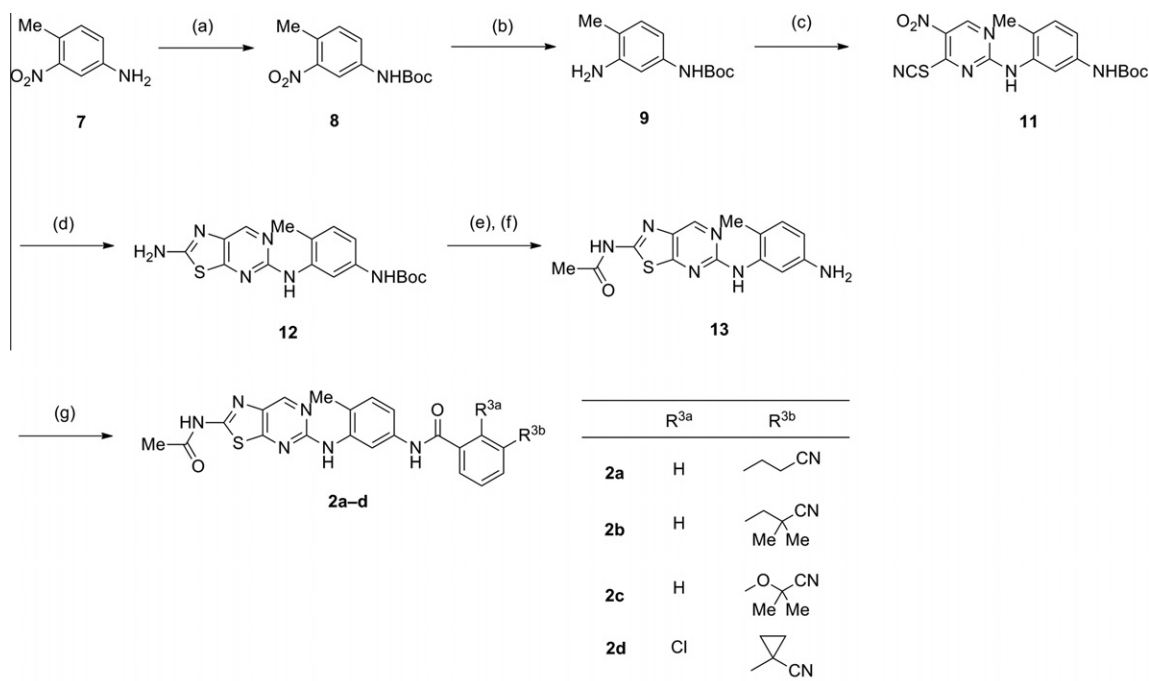
structure analysis of BRAF with **1**, the 1-cyanocyclopropyl group as R^{3b} occupies the hydrophobic ‘back pocket’ region. We assumed that this region could be important to stabilize the DFG-out inactive conformation of BRAF. On the basis of this assumption, we expected that the introduction of dimethyl groups at the adjacent position of terminal nitrile (**2b,c**) would enhance cellular pMEK inhibition.

Next, we selected 2-fluoroanilide as ring B from compound **1** on the basis of our previous work,⁵ and examined 5-amino-linked [1,3]thiazolo[5,4-*b*]pyridine scaffold (**3–6**) for the first time to aspire for the enhancement of cellular inhibitory activity. We calculated a twisting effect derived from *N*-methylation at the R² position (**3–5**). *N*-Methyl analog showed larger dihedral angles between ring A (29.2°) and ring B (39.4°) than those of NH analog (20.3° and 21.9°, respectively) (Fig. 4). *N*-Methyl derivatives **3–5** were expected to show twisted conformation between ring A and B, similar to compound **2a–d**. This twisting effect of *N*-methylation on solubility and PK profiles was verified using demethylated compound **6**. Finally, to further increase the thermodynamic solubility of selected compound **5**, salt formation with various acids, such as hydrochloride (**5a**), sulfate (**5b**), and besylate (**5c**) were evaluated. We have described these details in this manuscript.

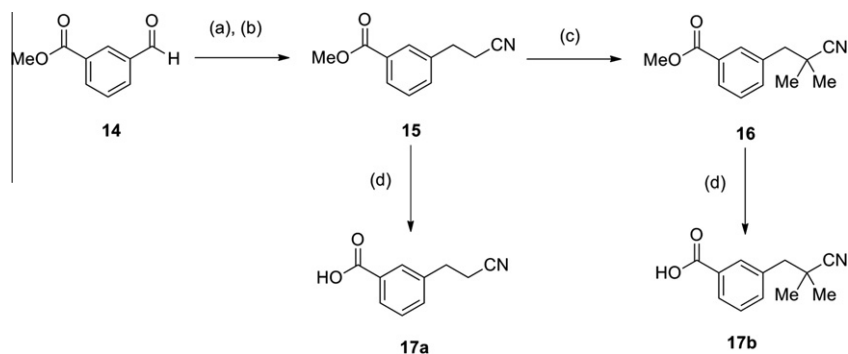
2. Chemistry

5-Amino-linked [1,3]thiazolo[5,4-*d*]pyrimidine¹¹ derivatives **2a–d** were synthesized by the route described in Scheme 1. Aniline protection of **7** by *tert*-butoxycarbonyl (Boc) group using Boc₂O provided *N*-Boc derivative **8** in 89% yield. Hydrogenation of the nitro group of **8** using 10% palladium on activated carbon (Pd/C) provided aniline **9**, which was reacted with commercially available 2-chloro-5-nitropyrimidin-4-yl thiocyanate **10** in the presence of *i*-Pr₂NEt in tetrahydrofuran (THF) to give **11** as a precursor molecule for [1,3]thiazolo[5,4-*d*]pyrimidine. Subsequent reduction of the nitro group of **11** using reduced iron (Fe(0)) in the presence of CaCl₂ resulted in ring formation reaction to afford [1,3]thiazolo[5,4-*d*]pyrimidine-2-amine derivative **12** in 35% yield in three steps. Acylation of **12** using acetyl chloride in pyridine (98% yield) followed by cleavage of *N*-Boc group using trifluoroacetic acid in anisole provided aniline **13** in 83% yield. Amide coupling reaction of **13** with various benzoic acids **17a–d** in the presence of *O*-(7-azabenzotriazol-1-yl)-*N,N,N',N'*-tetramethyluronium hexafluorophosphate (HATU) gave the target [1,3]thiazolo[5,4-*d*]pyrimidine derivatives **2a–d** in 46–65% yield.

The synthesis of 2-cyanoethylated and 2-cyano-2-methylpropylated benzoic acid (**17a, 17b**) is shown in Scheme 2.



Scheme 1. Reagents and conditions: (a) Boc₂O, THF, 70 °C, 15 h (89%); (b) H₂, 10% Pd/C, EtOH, THF, room temp, 22 h; (c) 2-chloro-5-nitropyrimidin-4-yl thiocyanate **10**, *i*-Pr₂NEt, THF, room temp, 30 min; (d) Fe(0), CaCl₂, NMP, EtOH, water, 100 °C, 16 h (35% in three steps); (e) AcCl, pyridine, room temp, 1 h (98%); (f) TFA, anisole, 0 °C, 1 h (83%); (g) benzoic acids, HATU, pyridine, room temp; (46–65%).



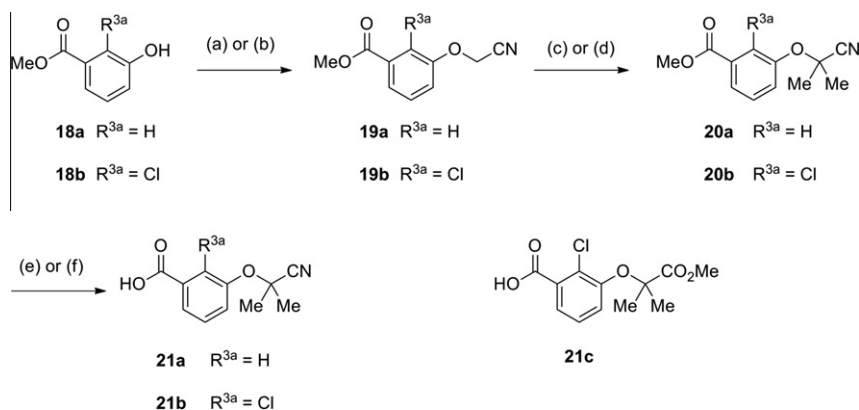
Scheme 2. Reagents and conditions: (a) diethyl (cyanomethyl) phosphonate, K_2CO_3 , THF, H_2O , 60 °C, 1 h; (b) H_2 , 10% Pd/C, EtOH, THF, room temp, 2 h (88% in two steps); (c) MeI, LHMDS, THF, –78 °C, 1 h (44%); (d) 2 N NaOH aq, MeOH, THF, 60 °C, 4 h (95–96%).

Horner–Wadsworth–Emmons reaction¹² of the commercially available formyl derivative **14** with diethyl (cyanomethyl) phosphonate in the presence of K_2CO_3 followed by hydrogenation of double bond using 10% Pd/C provided the cyanoethylated benzoate **15** in 88% yield in two steps. Dimethylation of the α -position of the cyano group in **15** was accomplished with MeI and lithium hexamethyldisilazide (LHMDS) under –78 °C conditions to give 3-(2-cyano-2-methylpropyl)benzoate **16** in 44% yield. Hydrolysis of **15**, **16** with aqueous 2 N NaOH provided **17a,b** in 95–96% yield.

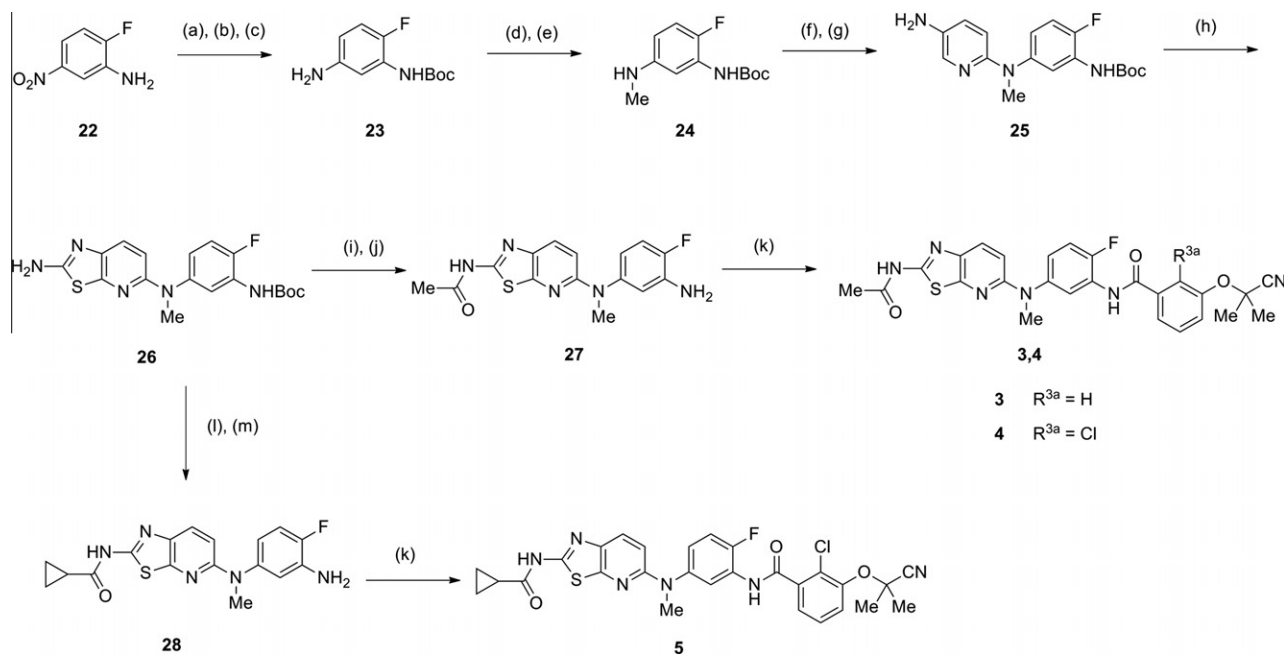
Phenoxy derivatives **21a,b** were prepared from the corresponding phenol derivatives **18a,b** as described in Scheme 3. Cyanomethylation of the phenolic hydroxy group in **18a** with bromoacetonitrile in the presence of K_2CO_3 provided **19a** in 86% yield. Dimethylation of the α -position of the cyano group in **19a** was achieved under conditions similar to those of **16** in Scheme 2. Compound **20a** was obtained in 30% yield. Hydrolysis of **20a** with aqueous 2 N NaOH in a mixed solvent of MeOH/THF (3:1) provided the target benzoic acid **21a** in 51% yield. Chlorinated derivative **21b** was prepared under reaction conditions similar to those used for the preparation for **21a**. However, the yields for each step were low. The optimized reaction conditions in a dozen gram-scale preparation are also described in Scheme 3. Starting from methyl 2-chloro-3-hydroxybenzoate **18b**, alkylation of the hydroxy group with chloroacetonitrile in the presence of K_2CO_3 and NaI gave the cyanomethylated compound **19b** in 92% yield. In the next dimethylation, the base used was changed from LHMDS to sodium hexamethyldisilazide (NaHMDS). The reaction proceeded smoothly at between 0 and 20 °C to give **20b** in 50% yield. Subsequent hydrolysis of methyl ester in **20b** gave **21b** in

less than 50% yield under the same conditions as that of **20a**. The production of methoxycarbonylated compound **21c** was detected in 1H NMR as a byproduct. We assumed that methanolysis of aliphatic nitrile may occur in competition with hydrolysis of methyl benzoate. To reduce the formation of **21c**, *i*-PrOH, a bulkier alcohol than MeOH, was used as a solvent. *i*-PrOH significantly reduced side reaction, and these reaction conditions gave **21b** as crystals in 77% yield after recrystallization from EtOH/ H_2O (1:2).

The synthesis of *N*-methyl [1,3]thiazolo[5,4-*b*]pyridine derivatives **3–5** is shown in Scheme 4. Boc introduction of 2-fluoro-5-nitroaniline **22** with Boc_2O in THF at 70 °C under reflux conditions was found to be slow, and the reaction was not completed even after 19 h. Because the nucleophilicity of aniline group was weak, we performed the reaction under modified neat conditions at 80 °C. The reaction proceeded smoothly, but resulted in a mixture of mono-Boc and di-Boc derivatives. Without purification, this mixture was subjected to hydrogenation reaction of nitro groups in the presence of 10% Pd/C to give the corresponding aniline derivatives. Subsequent treatment of the mixed aniline derivatives with K_2CO_3 resulted in conversion of di-Boc to mono-Boc to give compound **23** in 63% yield in three steps as a single product. Treatment of **23** with formic acid in the presence of acetic anhydride gave the corresponding formamide followed by reduction with boran dimethylsulfide complex to give monomethylated compound **24** in 73% yield in two steps. The reaction of **24** with commercially available 2-chloro-5-nitropyridine in DMSO provided a coupled product in 42% yield. Reduction of the nitro group under hydrogenation conditions afforded the corresponding aniline **25** in 87% yield. Fused 1,3-thiazolo ring was constructed by reaction of



Scheme 3. Reagents and conditions: (a) bromoacetonitrile, K_2CO_3 , acetone, reflux, 4 h (86%); (b) chloroacetonitrile, K_2CO_3 , NaI, acetone, reflux, 13 h (92%); (c) MeI, LHMDS, THF, –78 °C, 2 h, (30%); (d) MeI, NaHMDS, THF, room temp, 30 min (50%); (e) 2 N NaOH aq, MeOH, THF, room temp, 30 min (51%); (f) 2 N NaOH aq, *i*-PrOH, room temp, 2 h (77%).

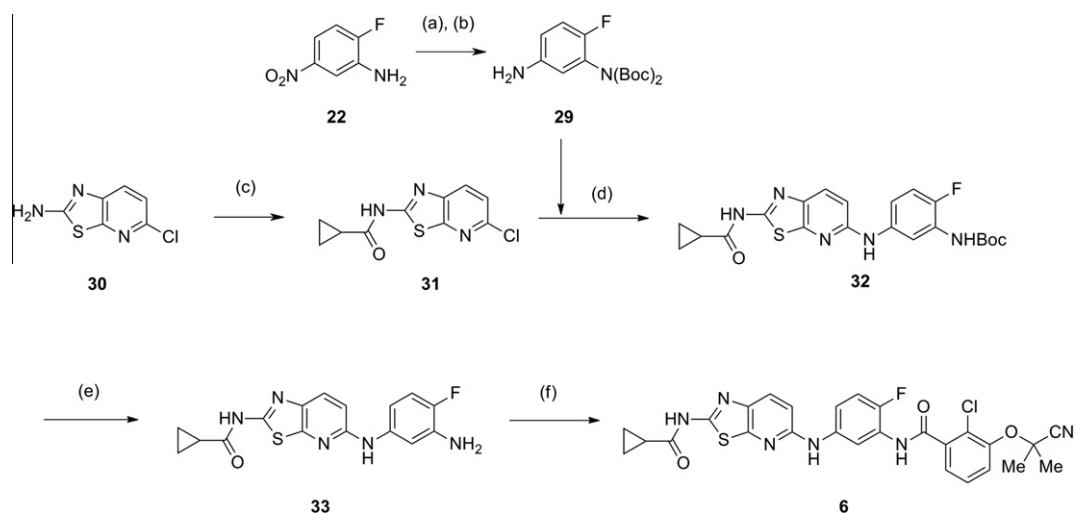


Scheme 4. Reagents and conditions: (a) Boc_2O , 80 °C, 24 h; (b) H_2 (1 atm), 10% Pd/C, EtOH, THF, room temp, 24 h; (c) K_2CO_3 , MeOH, THF, 60 °C, 4 h (63% in three steps); (d) Ac_2O , HCO_2H , THF, room temp, 16 h; (e) $BH_3 \cdot SMe_2$, THF, room temp, 1.5 h (73% in two steps); (f) 2-chloro-5-nitropyridine, DMSO, 60 °C, 19 h (42%); (g) H_2 (1 atm), 10% Pd/C, EtOH, THF, room temp, 16 h (87%); (h) KSCN, Br_2 , AcOH, room temp, 1.5 h (48%); (i) $AcCl$, pyridine, room temp, 30 min; (j) TFA, anisole, 0 °C, 1 h (86% in two steps); (k) **21a,b**, HATU, pyridine, 90 °C, 48–59%; (l) cyclopropanecarbonyl chloride, pyridine, room temp, 1 h; (m) TFA, anisole, 0 °C, 1 h (75% in two steps).

aniline **25** with potassium thiocyanate and bromine in AcOH to give the [1,3]thiazolo[5,4-*b*]pyridine derivative **26** in 48% yield. Acetylation of the 2-amino group of **26** with acetyl chloride in pyridine, followed by deprotection of the Boc group with trifluoroacetic acid (TFA) in the presence of anisole, gave the precursor amine **27** for introducing benzamide moieties, in 86% yield in two steps. Condensation of **27** with carboxylic acid **21a,b** using HATU in pyridine provided the desired [1,3]thiazolo[5,4-*b*]pyridine-2-acetamide derivatives **3,4** in 48–59% yield. The 2-cyclopropanecarboxamide derivative **5** was synthesized in a similar manner. Acylation of the 2-amino group in **26** with cyclopropanecarbonyl chloride in pyridine, followed by deprotection of the Boc group with TFA and anisole, afforded the aniline derivative **28** in

80% yield in two steps. Condensation reaction of **28** with carboxylic acid **21b** provided **5** in 50% yield.

The synthesis of **6** was performed as shown in Scheme 5. Boc introduction of aniline **22** was performed at 55 °C using 4 equiv of Boc_2O in the presence of Et_3N to give the corresponding di-Boc compound in 72% yield. The following reduction of the nitro group under hydrogenation conditions gave **29** in 64% yield. The commercially available [1,3]thiazolo[5,4-*b*]pyridine-2-amine **30** was acylated with cyclopropanecarbonyl chloride to give **31** in 30% yield. Next, Buchwald–Hartwig reaction¹³ of **31** with aniline **29** using $Pd_2(dba)_3$ and X-phos in the presence of *tert*-BuOK was performed under microwave irradiation. During this reaction, one Boc group of the di-Boc imide was cleaved to give the mono-Boc



Scheme 5. Reagents and conditions: (a) Boc_2O , Et_3N , CH_2Cl_2 , 55 °C, 12 h (72%); (b) 10% Pd/C, H_2 , MeOH, room temp, 12 h (64%); (c) cyclopropanecarbonyl chloride, THF, 0 °C, 2 h (30%); (d) $Pd_2(dba)_3$, X-phos, *tert*-BuOK, *tert*-BuOH, microwave, 90 °C, 35 min (63%); (e) 4 N HCl/EtOAc, 0 °C, 12 h (65%); (f) **21b**, $(COCl)_2$, cat. DMF, room temp, 1 h, then **33**, DMA, room temp, 2 h (66%).

product **32** in 63% yield. Deprotection of the N-Boc group (**32**) with 4 N HCl/EtOAc gave the corresponding aniline **33** in 65% yield. Finally, condensation reaction of aniline **33** with acid chloride prepared by carboxylic acid **21b** using oxalyl chloride in the presence of catalytic DMF provided the desired derivative **6** in 66% yield.

3. Results and discussion

The structure activity relationships (SAR) of 5-amino-linked [1,3]thiazolo[5,4-*d*]pyrimidines **2a–d** possessing various substituents on the ring C are described in Table 1. Cyanoethylated derivative **2a** showed moderate BRAF inhibitory activity with IC₅₀ value of 51 nM, but weak cellular pMEK inhibitory activity (IC₅₀ >500 nM). Our initial medicinal chemistry strategy to enhance cellular activity was the introduction of dimethyl groups at the adjacent position of the terminal nitrile group in **2a** to enhance hydrophobic interaction at the back pocket region. (Fig. 3)

Dimethylation of the cyanoethyl group (**2b**) resulted in significantly increased cellular pMEK inhibitory activity with IC₅₀ value of 150 nM, despite a slight reduction of BRAF inhibitory activity. Next, to mask the metabolically labile benzylic methylene (**2b**) by the oxygen atom, 3-(1-cyano-1-methylethoxy) derivative **2c** was evaluated. Compound **2c** showed better metabolic stability against human microsomes with the clearance rate of –13 μL/min/mg, as we expected. Moreover, compound **2c** exhibited further enhancement of the cellular activity with IC₅₀ value of 88 nM together with increase of BRAF inhibition comparable to those of 2-chloro-3-(1-cyanocyclopropyl) derivative **2d**.

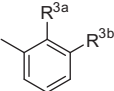
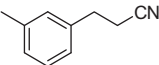
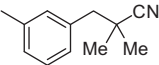
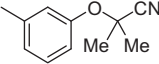
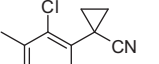
With an aim of further enhancement of cellular pMEK inhibitory activity, the finding of novel (1-cyano-1-methylethoxy) substituent (**2c**) triggered us to apply this functionality to 5-amino-linked [1,3]thiazolo[5,4-*b*]pyridine scaffold. The SAR of the [1,3]thiazolo[5,4-*b*]pyridine-5-amine derivatives **3–6** possessing the 3-(1-cyano-1-methylethoxy) group are shown in Table 2. The previous SAR study⁵ indicated that introduction of the fluorine atom at the 2-position of the benzanilide (ring B) was significant to block the metabolic labile site of ring B in the 5-oxy-linked

[1,3]thiazolo[5,4-*b*]pyridine derivatives along with maintaining the potent BRAF inhibition. Therefore, 2-fluorinated benzanilide was selected instead of 4-methyl benzanilide (**2a–d**), and we examined its adaptability to the 5-amino-linked chemotype. In addition, N-methyl linker was designed, and we attempted to achieve the twisted conformation between fused ring A and ring B to increase solubility.

The N-methyl [1,3]thiazolo[5,4-*b*]pyridine derivative **3** that we designed showed better BRAF and VEGFR2 inhibitory activity as well as more potent pMEK inhibitory activity with an IC₅₀ value of 30 nM than those of [1,3]thiazolo[5,4-*d*]pyrimidine **2c**. However, PK study indicated poor drug exposure of compound **3** with an AUC_{0–8h} value of 0.311 μg h/mL after oral administration at a dose of 10 mg/kg in mice. The introduction of a chlorine atom at the 2-position as an R^{3a} group enhanced the oral absorption on the basis of our empirical finding⁵, and thus, we attempted to apply our knowledge to compound **4**. Introduction of a chlorine atom at 2-position dramatically improved the oral absorption of compound **4** (AUC_{0–8h}, 14.308 μg h/mL) without decreasing the other desirable pharmacological effects. To achieve good PK profiles in humans, we explored the effects of replacement of acetamide (**4**, R¹ = Me) with cyclopropane carboxamide (**5**, R¹ = cPr). As we expected, compound **5** showed better metabolic stability (clearance rate: human 25 μL/min/mg, mouse 32 μL/min/mg) than acetamide **4**. In addition, compound **5** showed significant oral absorption with an AUC_{0–8h} value of 9.571 μg h/mL in mice. Pharmacological profiles of **5** (IC₅₀ values: BRAF, 38 nM; VEGFR2, 7.5 nM; and cellular pMEK, 47 nM) were almost comparable to those of compound **4**.

Finally, to verify the twisting effect of the N-methyl group on the physicochemical profiles of **5**, we evaluated the corresponding NH derivative **6**. Non-methylated derivative **6** showed significantly decreased AUC value (0.008 μg h/mL) because of its low thermodynamic solubility (0.91 μg/mL). Interestingly, N-methylation not only improved the oral PK profile of **6**, but also showed an eightfold increase in VEGFR2 inhibition (IC₅₀ values: **5**, 7.5 nM; **6**, 64 nM). Cellular VEGFR2 inhibitory activity was tested using HUVEC cells stimulated by VEGF. Compound **5** showed potent growth

Table 1
Structure-activity relationships of 5-amino-linked [1,3]thiazolo[5,4-*d*]pyrimidines **2a–d** possessing various ring C

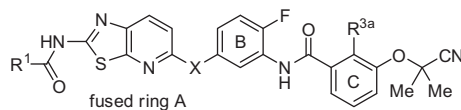
Compound		Kinase IC ₅₀ ^a (nM)		Cellular pMEK ^b IC ₅₀ (nM)	Human microsome stability ^c (μL/min/mg)
		BRAF (V600E)	VEGFR2		
2a		51	410	>500	35
2b		100	300	150	56
2c		73	510	88	-13
2d		91	340	120	73

^a n = 2.

^b Concentration producing 50% inhibition (IC₅₀) values against RAF substrate MEK phosphorylation in HT-29 (BRAF^{V600E} mutant) cultured human colon cancer cell lines.

^c Metabolism clearance of each compound was examined using human liver microsomes and NADPH.

Table 2
Profiles of 5-amino-linked [1,3]thiazolo[5,4-*b*]pyridines **3–6**



	R ¹	X	R ^{3a}	Kinase IC ₅₀ ^a (nM)		Cellular pMEK ^b IC ₅₀ (nM)	Microsome stability ^c (μL/min/mg)		Mouse PK ^d AUC PO (μg h/mL)
				BRAF (V600E)	VEGFR2		Human	Mouse	
3	Me	N-Me	H	23	10	30	22	25	0.311
4	Me	N-Me	Cl	45	14	22	45	55	14.308
5	cPr	N-Me	Cl	38	7.5	47	25	32	9.571
6	cPr	NH	Cl	15	64	87	N.D. ^e	N.D. ^e	0.008

^a *n* = 2.

^b Concentration producing 50% inhibition (IC₅₀) values against RAF substrate MEK phosphorylation in HT-29 (BRAF^{V600E} mutant) cultured human colon cancer cell lines.

^c Metabolism clearance of each compound was examined using liver microsomes and NADPH.

^d Mice cassette dosing of five compounds.

^e Not determined.

Table 3
Kinase selectivity of compound **5**

Kinase	IC ₅₀ ^a (nM)	Kinase	IC ₅₀ ^a (nM)
BRAF(wt)	69	PKA	>10,000
C-RAF	23	PKCθ	>10,000
FGFR3	86	CHK1	>10,000
PDGFRα	43	CK1δ	>10,000
PDGFRβ	91	ERK1	>10,000
EGFR	>10,000	CDK1	3700
Her2	1200	CDK2	>10,000
TIE2	840	Aurora B	4000
c-Met	>10,000	p38α	45
c-Kit	430	JNK1	>10,000
Src	130	GSK3β	>10,000
IR	>10,000	MEK1	1000
IKKβ	8100	MEKK1	>10,000

^a *n* = 2.

inhibition against HUVEC cells with IC₅₀ value of 1.2 nM. Thus, we selected compound **5**, characterized as a VEGFR2-dominant RAF/VEGFR2 inhibitor, for further development.

3.1. Kinase inhibitory profile of compound **5**

The inhibitory profiles of compound **5** against 26 different kinases are summarized in Table 3. The inhibitory activity of compound **5** against RAF family kinases, including BRAF(V600E), was comparable to that against the angiogenesis-related kinases such as FGFR3, PDGFRα, and PDGFRβ; range of IC₅₀ values, 23–91 nM. In addition, compound **5** inhibited p38α; IC₅₀ value, 45 nM. Several kinases, including Src, c-Kit, and Tie2 were moderately inhibited by compound **5**; range of IC₅₀ values, 130–840 nM. Further, no significant inhibition was observed against the remaining 17 kinases. Thus, compound **5** was considered a pan-RAF and angiogenesis-related kinases inhibitor characterized by dominant VEGFR2 inhibition (IC₅₀ = 7.5 nM).

3.2. X-ray co-crystal structural analysis of compound **5** with BRAF

The mode of binding of compound **5** to BRAF was determined by X-ray co-crystal structural analysis (Fig. 5).¹⁴ The results of the analysis revealed that compound **5** occupies the ATP-binding site and stabilizes the inactive 'DFG-out' conformation of BRAF. Thiazolo[5,4-*b*]pyridine-2-cyclopropanecarboxamide moiety anchors to the kinase hinge region by forming 2 hydrogen bonds between

the main chain atoms of Cys532 and the nitrogen atoms of carboxamide and fused-thiazolo ring, and presents planar conformation between the core scaffold (ring A) and carboxamide by carbonyl-sulfur interaction. The benzanilide moiety (ring B and ring C) anchors to DFG-out conformation of BRAF by forming 2 hydrogen bonds with the carboxylate of Glu501 from helix C and the backbone NH from Asp594 as a DFG motif. The novel 2-chloro-3-(1-cyano-1-methylethoxy)benzene moiety (ring C) occupies the hydrophobic back pocket lined by residues Val504, Leu505, Thr508, Ile513, Leu514, Leu567, His574, Ile592, and Gly593. These results are consistent with those of our initial design based on modeling.

3.3. Salt formation study of compound **5**

We investigated the ability of salt formation of compound **5** with optimal acids to enhance oral absorption along with improving solubility. Although 5-oxy-linked [1,3]thiazolo[5,4-*b*]pyridine derivative **1** did not form the salt, 5-amino-linked [1,3]thiazolo[5,4-*b*]pyridine derivative **5** formed salts with various acids. Among the salts, hydrochloride (**5a**), sulfate (**5b**), and besylate monohydrate (**5c**) were suitable forms for their characterization. Powder X-ray diffractometry (XRD) experiments revealed that these 3 salts formed crystalline state with crystallinity values of 42–81% (Table 4). Melting point of each compound was determined by differential scanning calorimetry (DSC). Melting points of 5-amino-linked derivative **5** (165 °C) and its salts **5a–c** (128–179 °C) were much lower than that of 5-oxy-linked derivative **1** (213 °C). The 5-amino-linked derivative **5** and its salts **5a–c** showed higher thermodynamic solubility¹⁵ than the 5-oxy-linked derivative **1** consistent with the above results. In particular, the thermodynamic solubility (31–37 μg/mL) of the 5-amino-linked derivative **5** was enhanced by salt formation (**5a–c**) compared to that of the free base **5** (18 μg/mL). The AUC_{0–8h} value of besylate monohydrate **5c** (23.246 μg h/mL) was the highest among the AUC_{0–8h} values of the other salts and therefore we selected **5c** as a promising candidate for further evaluation.

3.4. Pharmacokinetic profiles and in vivo studies of **5c** in rats

Oral administration of **5c** at a dose of 25 mg/kg showed good oral bioavailability (%F = 38.4%) with an AUC value of 5.77 μg h/mL in rats. Selected PK profiles of **5c** in rats are shown in Table 5.

We evaluated in vivo activity of compound **5c** in a HT-29 human colorectal cancer xenograft model in nude rats after oral

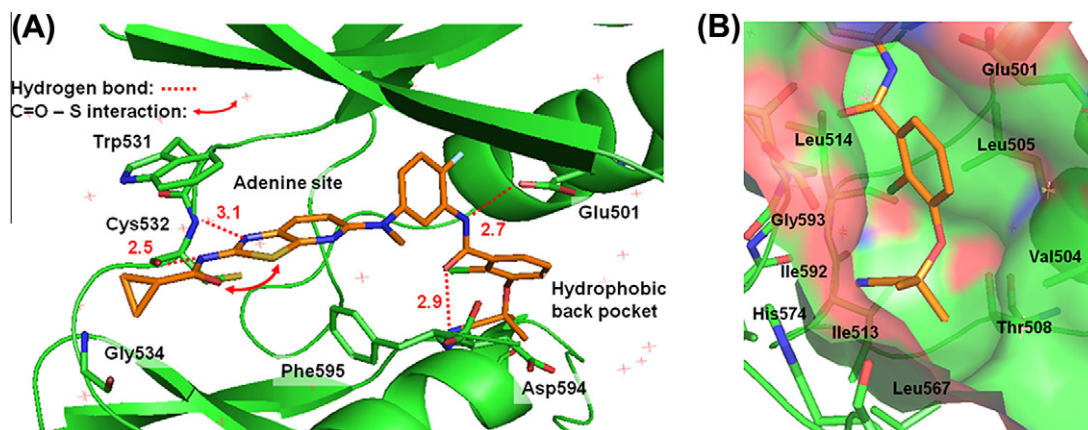


Figure 5. Crystal structure of compound **5** with BRAF (PDB code: 4FC0, 2.95 Å resolution). (A) DFG-out conformation of BRAF is stabilized by **5**. (B) Back pocket region of BRAF (surface).

Table 4

Selected physicochemical properties and pharmacokinetic profile of **5** and its salts **5a–c**, compared with **1**

Compound	Salt	Crystallinity ^a (%)	Melting point ^b (°C)	Thermodynamic solubility ^c (μg/mL)	Mouse PK ^d AUC PO (μg h/mL)
5	Free base	38	165	18	9.571
5a	Hydrochloride	56	164	31	19.846
5b	Sulfate	42	179	35	15.917
5c	Besylate·H ₂ O	81	128	37	23.246
1	Free base	55	213	3.6	1.902

^a Determined by powder X-ray diffractometry.

^b Determined by differential scanning calorimetry.

^c The Japanese Pharmacopoeia 2nd fluid for disintegration test (pH 6.8) (JP2)¹⁵ containing 20 mmol/L of bile acid.

^d Cassette dosing of five compounds. Values shown are mean of data from three mice. Compounds (10 mg/kg) were administered in 0.5% methylcellulose in distilled water.

Table 5

Mean^a pharmacokinetic parameters for **5c** in rats

Dose (mg/kg)	Route	CL _{total} (mL/h/kg)	V _{dss} (mL/kg)	MRT (h)	AUC _{0–24h} (μg h/mL)	C _{max} PO (μg/mL)	%F (%)
1 ^b	iv	1750 ± 433	5517 ± 1581	3.13 ± 0.23	0.60 ± 0.17		
25 ^c	Oral			5.26 ± 0.55	5.77 ± 2.97	0.66 ± 0.24	38.4 ± 19.9

^a Values shown are mean ± SD of data from 3 rats.

^b Delivered in polyethylene glycol:DMA (1/1).

^c Delivered in 0.5% methylcellulose in distilled water.

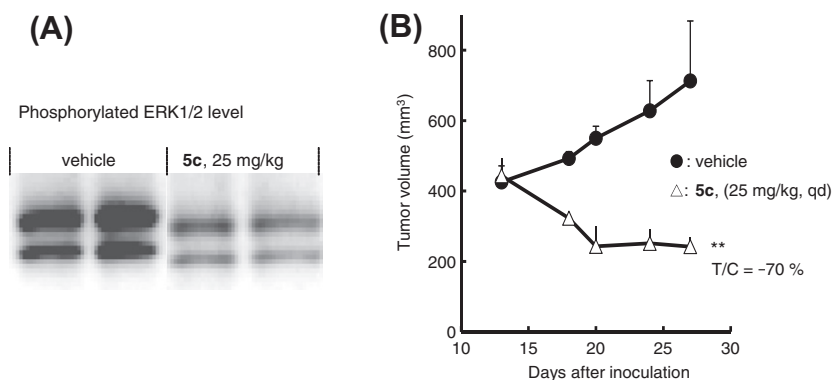


Figure 6. In vivo studies of **5c** (25 mg/kg, qd) in a BRAF(V600E) bearing HT-29 human colorectal cancer xenograft models in F344 nude rats. (A) The levels of phosphorylated ERK1/2 were reduced in tumor tissues ($n = 2$) in 4 h after treatment with single dose of 25 mg/kg of **5c**. (B) Antitumor efficacy of **5c** was determined ($n = 3$) at a dose of 25 mg/kg/day for consecutive 14 days. Data are plotted as mean tumor volume (in mm³) ± standard error of the mean, ** $P \leq 0.01$ versus control group at day 14 (t -test).

administration of **5c** at a dose of 25 mg/kg in a conventional 0.5% methylcellulose suspension. Reflecting the good oral PK profile based on improved solubility, compound **5c** significantly suppressed the phosphorylation of ERK on the basis of BRAF inhibition

in tumor tissues (Fig. 6A). Repetitive administration of **5c** at the same dose (25 mg/kg, qd) for 2 weeks showed tumor regression with T/C value of -70% without lethal toxicity (Fig. 6B). Because compound **5** showed a greater inhibition of VEGFR2 than that of

BRAF, we supposed that this strong antitumor efficacy would be achieved by the strong inhibition against both BRAF and VEGFR2.

4. Conclusion

We performed structure-guided drug design to determine DFG-out type RAF/VEGFR2 inhibitors that possess potent activity together with sufficient oral PK profiles. The binding mode analysis of *N*-methyl [1,3]thiazolo[5,4-*b*]pyridine derivative **5** validated by BRAF X-ray co-crystal structure revealed that the novel 2-chloro-3-(1-cyano-1-methylethoxy)benzene moiety (ring C) occupied the hydrophobic back pocket of BRAF. In addition, we found that *N*-methylation of the aniline moiety for twisting the conformation between fused ring A and ring B contributed not only to improving the solubility but also to enhancing the VEGFR2 inhibitory activity of **5**. On the basis of this effect, we characterized compound **5** as a VEGFR2-dominant RAF/VEGFR2 inhibitor. Salt formation of free base **5** with besylate monohydrate (**5c**) was identified by single X-ray crystallographic analysis. Compound **5c** showed better thermodynamic solubility and oral PK profile in mice than that of its free base **5** and other salts **5a,b**.

Pharmacokinetic evaluation of **5c** in rats showed significant oral absorption at a dose of 25 mg/kg. In a HT-29 human colorectal cancer xenograft model in nude rats, single administration of compound **5c** showed significant suppression of the phosphorylated ERK levels at a dose of 25 mg/kg. In the similar xenografted model, **5c** demonstrated tumor regression with a T/C value of $\sim 70\%$ by repetitive oral administration at a dose of 25 mg/kg, qd without lethal toxicity. We supposed that this potent antitumor efficacy of **5c** was achieved by the strong inhibitory activity against both BRAF and VEGFR2 on the basis of *in vitro* pharmacological profiles. Thus, compound **5c** was selected as a promising candidate of RAF/VEGFR2 inhibitor.

5. Experimental section

5.1. General chemistry information

The starting materials, reagents, and solvents for reactions were reagent-grade and were used as purchased. Thin-layer chromatography (TLC) was carried out using Merck Kieselgel 60, 63–200 mesh, F254 plates or Fuji Silysia Chemical Ltd., 100–200 mesh, NH plates. Chromatographic purification was carried out using silica gel (Merck, 70–230 mesh) or basic silica gel (Fuji Silysia Chemical Ltd, DM1020, 100–200 mesh). Melting points were obtained using an OptiMelt melting point apparatus MPA100 and used uncorrected. Proton nuclear magnetic resonance ^1H NMR spectra were recorded using a Bruker AVANCE II (300 MHz) spectrometer with tetramethylsilane (TMS) as an internal standard. The NMR data are given as follows: chemical shift (δ) in ppm, multiplicity (where applicable), coupling constants (*J*) in Hz (where applicable), and integration (where applicable). Multiplicities are indicated by s (singlet), d (doublet), t (triplet), q (quartet), dd (double doublets), dt, (double triplet), ddd (double double doublet), br s (broad singlet), or m (multiplet). MS spectra were collected with a Waters LC–MS system (ZMD-1) and were used to confirm $\geq 95\%$ purity of each compound. The column used was an L-column 2 ODS (3.0 \times 50 mm I.D., CERI, Japan) with a temperature of 40 $^\circ\text{C}$ and a flow rate of 1.2 mL/min. Mobile phase A was 0.05% TFA in ultrapure water. Mobile phase B was 0.05% TFA in acetonitrile which was increased linearly from 5% to 90% over 2 min, 90% over the next 1.5 min, after which the column was equilibrated to 5% for 0.5 min. Elemental analyses (Anal.) and high-resolution mass spectroscopy (HRMS) were carried out at Takeda Analytical Laboratories, Ltd Yields were not optimized.

5.2. *N*-(3-[[2-(Acetylamino)[1,3]thiazolo[5,4-*d*]pyrimidin-5-yl]amino]-4-methylphenyl)-3-(2-cyanoethyl) benzamide (**2a**)

To a mixture of 3-(2-cyanoethyl)benzoic acid **17a** (74 mg, 0.420 mmol) and HATU (160 mg, 0.420 mmol) in pyridine (4 mL) was added **13** (120 mg, 0.38 mmol) at room temperature. The mixture was stirred at room temperature for 1 h. It was then partitioned between EtOAc (20 mL) and aqueous NaHCO_3 solution (15 mL). The aqueous layer was extracted with EtOAc (5 mL). The combined organic layer was washed with brine (5 mL), dried over anhydrous Na_2SO_4 and concentrated *in vacuo*. The resulting residue was purified with basic silica gel column chromatography (12 g, 70–100% EtOAc in *n*-hexane) to give **2a** (117 mg, 65%) as pale yellow amorphous solid: ^1H NMR (300 MHz, $\text{DMSO-}d_6$) δ 2.19 (3H, s), 2.19 (3H, s), 2.83–2.92 (2H, m), 2.94–3.04 (2H, m), 7.20 (1H, d, *J* = 8.7 Hz), 7.44–7.56 (3H, m), 7.79–7.88 (2H, m), 7.92 (1H, d, *J* = 2.1 Hz), 8.75 (1H, s), 9.00 (1H, br s), 10.17 (1H, br s), 12.35 (1H, br s). HRMS (ESI): Calcd for $\text{C}_{24}\text{H}_{21}\text{N}_7\text{O}_2\text{S}$ [M+H] $^+$ 472.1550. Found: 472.1521.

5.3. *N*-(3-[[2-(Acetylamino)[1,3]thiazolo[5,4-*d*]pyrimidin-5-yl]amino]-4-methylphenyl)-3-(2-cyano-2-methylpropyl)benzamide (**2b**)

Compound **2b** (108 mg) was prepared from **13** (120 mg, 0.382 mmol), 3-(2-cyano-2-methylpropyl)benzoic acid **17b** (86 mg, 0.420 mmol) and HATU (160 mg, 0.420 mmol) by the method similar to that described for **2a**. Yield: 56%; colorless crystals; recrystallized from MeOH; mp 289–290 $^\circ\text{C}$. ^1H NMR (300 MHz, $\text{DMSO-}d_6$) δ 1.33 (6H, s), 2.19 (3H, s), 2.19 (3H, s), 2.94 (2H, s), 7.20 (1H, d, *J* = 8.5 Hz), 7.46–7.57 (3H, m), 7.83 (1H, s), 7.85–7.91 (1H, m), 7.92 (1H, d, *J* = 2.3 Hz), 8.74 (1H, s), 8.99 (1H, br s), 10.19 (1H, br s), 12.35 (1H, br s). HRMS (ESI): Calcd for $\text{C}_{26}\text{H}_{25}\text{N}_7\text{O}_2\text{S}$ [M+H] $^+$ 500.1863. Found: 500.1836.

5.4. *N*-(3-[[2-(Acetylamino)[1,3]thiazolo[5,4-*d*]pyrimidin-5-yl]amino]-4-methylphenyl)-3-(1-cyano-1-methylethoxy)benzamide (**2c**)

Compound **2c** (61 mg) was prepared from **13** (83 mg, 0.265 mmol), 3-(1-cyano-1-methylethoxy)benzoic acid **21a** (85 mg, 0.345 mmol) and HATU (120 mg, 0.318 mmol) by the method similar to that described for **2a**. Yield: 46%; colorless crystals; recrystallized from THF/*n*-hexane; mp 276–277 $^\circ\text{C}$. ^1H NMR (300 MHz, $\text{DMSO-}d_6$) δ 1.74 (6H, s), 2.19 (3H, s), 2.19 (3H, s), 7.20 (1H, d, *J* = 8.4 Hz), 7.40 (1H, ddd, *J* = 8.0, 2.3, 1.1 Hz), 7.51 (1H, dd, *J* = 8.4, 2.1 Hz), 7.56 (1H, t, *J* = 8.0 Hz), 7.70 (1H, t, *J* = 2.3 Hz), 7.79 (1H, dt, *J* = 8.0, 1.1 Hz), 7.92 (1H, d, *J* = 2.1 Hz), 8.74 (1H, s), 9.00 (1H, br s), 10.24 (1H, br s), 12.35 (1H, br s). HRMS (ESI): Calcd for $\text{C}_{25}\text{H}_{23}\text{N}_7\text{O}_3\text{S}$ [M+H] $^+$ 502.1656. Found: 502.1623.

5.5. *N*-(3-[[2-(Acetylamino)[1,3]thiazolo[5,4-*d*]pyrimidin-5-yl]amino]-4-methylphenyl)-2-chloro-3-(1-cyanocyclopropyl)benzamide (**2d**)

Compound **2d** (121 mg) was prepared from **13** (120 mg, 0.382 mmol), 2-chloro-3-(1-cyanocyclopropyl)benzoic acid (110 mg, 0.500 mmol) and HATU (189 mg, 0.500 mmol) by the method similar to that described for **2a**. Yield: 61%; off-white crystals; recrystallized from EtOAc; mp 264–266 $^\circ\text{C}$. ^1H NMR (300 MHz, $\text{DMSO-}d_6$) δ 1.40–1.51 (2H, m), 1.74–1.86 (2H, m), 2.18 (3H, s), 2.19 (3H, s), 7.20 (1H, d, *J* = 8.3 Hz), 7.41–7.53 (2H, m), 7.59 (1H, dd, *J* = 7.8, 1.8 Hz), 7.64 (1H, dd, *J* = 7.6, 1.8 Hz), 7.90 (1H, d, *J* = 2.1 Hz), 8.73 (1H, s), 8.98 (1H, br s), 10.50 (1H, br s), 12.35 (1H, br s). HRMS (ESI): Calcd for $\text{C}_{25}\text{H}_{20}\text{ClN}_7\text{O}_2\text{S}$ [M+H] $^+$ 518.1160. Found: 518.1125.

5.6. *N*-[5-[[2-(Acetylamino)[1,3]thiazolo[5,4-*b*]pyridin-5-yl](methyl)amino]-2-fluorophenyl]-3-(1-cyano-1-methylethoxy)benzamide (3)

Compound **3** (61 mg) was prepared from **27** (80 mg, 0.241 mmol), **21a** (99 mg, 0.482 mmol) and HATU (183 mg, 0.482 mmol) by the method similar to that described for **2a**. Yield: 48%; off-white crystals; recrystallized from THF/*n*-hexane; mp 203–204 °C. ¹H NMR (300 MHz, DMSO-*d*₆) δ 1.74 (6H, s), 2.17 (3H, s), 3.43 (3H, s), 6.63 (1H, d, *J* = 8.9 Hz), 7.24 (1H, ddd, *J* = 8.9, 4.5, 2.7 Hz), 7.39 (1H, dd, *J* = 10.2, 8.9 Hz), 7.43 (1H, ddd, *J* = 8.0, 2.5, 0.9 Hz), 7.57 (1H, t, *J* = 8.0 Hz), 7.60 (1H, dd, *J* = 6.9, 2.7 Hz), 7.73 (1H, t, *J* = 1.9 Hz), 7.75–7.85 (2H, m), 10.26 (1H, br s), 12.16 (1H, br s). Anal. Calcd for C₂₆H₂₃FN₆O₃S: C, 60.22; H, 4.47; N, 16.21. Found: C, 60.18; H, 4.53; N, 16.16. HRMS (ESI): Calcd for C₂₆H₂₃FN₆O₃S [M+H]⁺ 519.1609. Found: 519.1594.

5.7. *N*-[5-[[2-(Acetylamino)[1,3]thiazolo[5,4-*b*]pyridin-5-yl](methyl)amino]-2-fluorophenyl]-2-chloro-3-(1-cyano-1-methylethoxy)benzamide (4)

Compound **4** (78 mg) was prepared from **27** (80 mg, 0.241 mmol), **21b** (133 mg, 0.554 mmol) and HATU (211 mg, 0.554 mmol) by the method similar to that described for **2a**. Yield: 59%; off-white crystals; recrystallized from EtOH; mp 181–182 °C. ¹H NMR (300 MHz, DMSO-*d*₆) δ 1.79 (6H, s), 2.17 (3H, s), 3.43 (3H, s), 6.64 (1H, d, *J* = 9.1 Hz), 7.21 (1H, ddd, *J* = 8.7, 4.0, 2.7 Hz), 7.34–7.42 (2H, m), 7.50 (1H, t, *J* = 8.0 Hz), 7.58 (1H, dd, *J* = 8.0, 1.6 Hz), 7.79 (1H, d, *J* = 9.1 Hz), 7.85 (1H, dd, *J* = 6.9, 2.7 Hz), 10.50 (1H, br s), 12.17 (1H, br s). Anal. Calcd for C₂₆H₂₂ClFN₆O₃S+0.5H₂O: C, 55.56; H, 4.12; N, 14.95. Found: C, 55.76; H, 4.04; N, 14.91.

5.8. 2-Chloro-3-(1-cyano-1-methylethoxy)-*N*-[5-[[2-[(cyclopropylcarbonyl)amino][1,3]thiazolo[5,4-*b*]pyridin-5-yl](methyl)amino]-2-fluorophenyl]benzamide (5)

Compound **5** (123 mg) was prepared from **28** (150 mg, 0.420 mmol), 2-chloro-3-(1-cyano-1-methylethoxy)benzoic acid **21b** (201 mg, 0.840 mmol) and HATU (319 mg, 0.840 mmol) by the method similar to that described for **2a**. Yield: 50%; colorless crystals; recrystallized from EtOAc; mp 178–179 °C. ¹H NMR (300 MHz, DMSO-*d*₆) δ 0.89–0.99 (4H, m), 1.92–2.03 (1H, m), 3.43 (3H, s), 6.64 (1H, d, *J* = 8.9 Hz), 7.20 (1H, ddd, *J* = 8.9, 4.2, 2.8 Hz), 7.34–7.42 (2H, m), 7.50 (1H, t, *J* = 8.0 Hz), 7.58 (1H, dd, *J* = 8.0, 1.5 Hz), 7.79 (1H, d, *J* = 8.9 Hz), 7.85 (1H, dd, *J* = 7.0, 2.8 Hz), 10.50 (1H, br s), 12.46 (1H, br s). Anal. Calcd for C₂₈H₂₄ClFN₆O₃S: C, 58.08; H, 4.06; N, 14.51. Found: C, 57.81; H, 4.06; N, 14.45. HRMS (ESI): Calcd for C₂₈H₂₄ClFN₆O₃S [M + H]⁺ 579.1376. Found: 579.1337. Powder X-ray diffraction (Cu-Kα radiation, diffraction angle: 2θ(°)): 2.78, 8.46, 10.90, 11.34, 12.64, 13.66, 14.22, 22.94.

5.9. 2-Chloro-3-(1-cyano-1-methylethoxy)-*N*-[5-[[2-[(cyclopropylcarbonyl)amino][1,3]thiazolo[5,4-*b*]pyridin-5-yl](methyl)amino]-2-fluorophenyl]benzamide hydrochloride (5a)

To a solution of **5** (100 mg, 0.173 mmol) in a mixed solvent of EtOAc (8 mL) and EtOH (20 mL) was added 4 N HCl/EtOAc (88 μL, 0.352 mmol) at 50 °C. The mixture was stirred at room temperature for 30 min. It was then evaporated under reduced pressure. The residue was triturated with EtOH for 2 h, and the precipitate was collected by filtration to give **5a** (78.8 mg, 74%) as colorless crystals. ¹H NMR (300 MHz, DMSO-*d*₆) δ 0.77–1.05 (4H, m), 1.79 (6H, s), 1.89–2.07 (1H, m), 3.43 (3H, s), 6.64 (1H, d, *J* = 9.0 Hz), 7.12–7.30 (1H, m), 7.32–7.44 (2H, m), 7.50 (1H, t, *J* = 7.8 Hz),

7.54–7.62 (1H, m), 7.79 (1H, d, *J* = 9.0 Hz), 7.85 (1H, dd, *J* = 6.9, 2.7 Hz), 10.51 (1H, s), 12.48 (1H, s). Anal. Calcd for C₂₈H₂₅Cl₂FN₆O₃S: C, 54.64; H, 4.09; N, 13.65; Cl, 11.52. Found: C, 54.66; H, 3.98; N, 13.63; Cl, 11.32. Powder X-ray diffraction (Cu-Kα radiation, diffraction angle: 2θ(°)): 4.08, 14.06, 16.22, 18.22, 18.60, 21.06, 23.08, 23.54, 23.92, 24.06, 25.34.

5.10. 2-Chloro-3-(1-cyano-1-methylethoxy)-*N*-[5-[[2-[(cyclopropylcarbonyl)amino][1,3]thiazolo[5,4-*b*]pyridin-5-yl](methyl)amino]-2-fluorophenyl]benzamide sulfate (5b)

To a mixture of sulfuric acid (26.5 μL, 0.518 mmol) in *n*-heptane (6 mL) was added a solution of **5** (150 mg, 0.259 mmol) in EtOAc (6 mL). The mixture was diluted with EtOAc (12 mL) and stirred at 50 °C for 30 min. It was then evaporated under reduced pressure. The residue was recrystallized from THF/*n*-heptane (1:1, 20 mL). The precipitate was collected by filtration to give **5b** (140 mg, 80%) as pale yellow crystals. ¹H NMR (300 MHz, DMSO-*d*₆) δ 0.74–1.06 (4H, m), 1.79 (6H, s), 1.92–2.09 (1H, m), 3.43 (3H, s), 6.64 (1H, d, *J* = 8.9 Hz), 7.16–7.24 (1H, m), 7.33–7.65 (4H, m), 7.79 (1H, d, *J* = 8.9 Hz), 7.85 (1H, dd, *J* = 6.9, 2.5 Hz), 10.51 (1H, s), 12.47 (1H, s). Anal. Calcd for C₂₈H₂₄ClFN₆O₃S+1.0H₂SO₄: C, 49.67; H, 3.87; N, 12.41. Found: C, 49.27; H, 3.91; N, 12.18. Powder X-ray diffraction (Cu-Kα radiation, diffraction angle: 2θ(°)): 3.72, 11.38, 13.64, 18.14, 18.80, 19.04, 23.00.

5.11. 2-Chloro-3-(1-cyano-1-methylethoxy)-*N*-[5-[[2-[(cyclopropylcarbonyl)amino][1,3]thiazolo[5,4-*b*]pyridin-5-yl](methyl)amino]-2-fluorophenyl]benzamide besylate hydrate (5c)

To a solution of **5** (4.17 g, 7.20 mmol) in EtOAc (55 mL) was added a solution of benzenesulfonic acid (90%, 1.52 g, 8.64 mmol) in EtOAc (5 mL) at 55 °C. It was then cooled and evaporated under reduced pressure. The residue was crystallized from THF/*n*-heptane (1:1, 100 mL) to give crude besylate salt (5.02 g). The resulting crude salt was recrystallized from a mixed solvent of acetone (115 mL) and *n*-heptane (100 mL), and the resulting precipitate was collected by filtration to give **5c** (4.59 g, 84%) as colorless crystals. ¹H NMR (300 MHz, DMSO-*d*₆) δ 0.73–1.08 (4H, m), 1.79 (6H, s), 1.90–2.08 (1H, m), 3.43 (3H, s), 6.64 (1H, d, *J* = 9.0 Hz), 7.13–7.25 (1H, m), 7.25–7.45 (5H, m), 7.50 (1H, t, *J* = 7.8 Hz), 7.54–7.64 (3H, m), 7.79 (1H, d, *J* = 9.0 Hz), 7.85 (1H, dd, *J* = 7.0, 2.6 Hz), 10.50 (1H, s), 12.47 (1H, s). Anal. Calcd for C₃₄H₃₀ClFN₆O₆S₂+1.0H₂O: C, 54.07; H, 4.27; N, 11.13. Found: C, 54.03; H, 4.31; N, 11.08. Powder X-ray diffraction (Cu-Kα radiation, diffraction angle: 2θ(°)): 4.08, 8.28, 12.50, 16.54, 21.00, 23.36, 24.62.

5.12. 2-Chloro-3-(1-cyano-1-methylethoxy)-*N*-[5-[[2-[(cyclopropylcarbonyl)amino][1,3]thiazolo[5,4-*b*]pyridin-5-yl]amino]-2-fluorophenyl]benzamide (6)

To a solution of **21b** (278 mg, 1.16 mmol) in THF (2.5 mL) were added DMF (25 μL) and oxalyl chloride (125 μL, 1.46 mmol), and the mixture was stirred at room temperature for 1 h. The reaction mixture was concentrated under reduced pressure to give 2-chloro-3-(1-cyano-1-methylethoxy)benzoyl chloride as pale yellow oil. To a solution of 2-chloro-3-(1-cyano-1-methylethoxy)benzoyl chloride in DMA (4.0 mL) was added **33** (200 mg, 0.582 mmol), and the mixture was stirred at room temperature for 2 h. To the reaction mixture was added saturated aqueous NaHCO₃ (20 mL), and the mixture was extracted with EtOAc (50 mL). The organic layer was washed with water (20 mL) and brine (20 mL), and dried over anhydrous Na₂SO₄, and concentrated under reduced pressure. The residue was purified by silica gel column chromatography (20–100% EtOAc in *n*-hexane) and crystallized from *n*-hexane/EtOAc (1:1) to give **6** (216 mg, 66%) as pale purple crystals: mp

226–228 °C. ¹H NMR (DMSO-*d*₆) δ 0.86–1.00 (4H, m), 1.80 (6H, s), 1.91–2.04 (1H, m), 6.92 (1H, d, *J* = 8.9 Hz), 7.20 (1H, t, *J* = 10.2, 9.3 Hz), 7.39 (1H, dd, *J* = 7.0, 1.5 Hz), 7.46–7.63 (2H, m), 7.63–7.73 (1H, m), 7.90 (1H, d, *J* = 8.9 Hz), 8.16 (1H, dd, *J* = 7.0, 2.7 Hz), 9.40 (1H, s), 10.35 (1H, s), 12.47 (1H, br s). Anal. Calcd for C₂₇H₂₂ClFN₆O₃S: C, 57.39, H, 3.92, N, 14.87. Found: C, 57.34; H, 3.99; N, 14.69. HRMS (ESI): Calcd for C₂₇H₂₂ClFN₆O₃S [M+H]⁺ 565.1219. Found: 565.1198.

5.13. *tert*-Butyl (4-methyl-3-nitrophenyl)carbamate (8)

To a solution of 4-methyl-3-nitroaniline **7** (15.0 g, 98.6 mmol) in THF (40 mL) was added dropwise Boc₂O (25.8 g, 118 mmol) in THF (20 mL) over 30 min at 70 °C. The reaction mixture was stirred at 70 °C for 15 h and concentrated under reduced pressure. The resulting residue was recrystallized with EtOAc/*n*-hexane to give compound **8** (22.3 g, 89%) as pale yellow crystals; mp 86–87 °C. ¹H NMR (300 MHz, DMSO-*d*₆) δ 1.48 (9H, s), 2.43 (3H, s), 7.38 (1H, d, *J* = 8.6 Hz), 7.58 (1H, dd, *J* = 8.6, 2.3 Hz), 8.22 (1H, d, *J* = 2.3 Hz), 9.76 (1H, br s). Anal. Calcd for C₁₂H₁₆N₂O₄: C, 57.13; H, 6.39; N, 11.10. Found: C, 57.31; H, 6.46; N, 11.22.

5.14. *tert*-Butyl {3-[(2-amino[1,3]thiazolo[5,4-*d*]pyrimidin-5-yl)amino]-4-methylphenyl}carbamate (12)

To a solution of **8** (10.1 g, 39.8 mmol) in EtOH (60 mL) and THF (20 mL) was added 10% Pd/C (2.12 g). The mixture was stirred at room temperature for 22 h under H₂ atmosphere (3 atm). The mixture was diluted with EtOAc (80 mL) and passed through a pad of Celite. The filtrate was concentrated in vacuo to give *tert*-butyl (3-amino-4-methylphenyl) carbamate **9** as colorless solid (8.82 g). This material was used for the next reaction without further purification. ¹H NMR (300 MHz, DMSO-*d*₆) δ 1.44 (9H, s), 1.95 (3H, s), 4.72 (2H, br s), 6.48 (1H, d, *J* = 7.9 Hz), 6.73 (1H, d, *J* = 7.9 Hz), 6.82 (1H, s), 8.90 (1H, br s).

To a solution of **9** in THF (200 mL) were added *i*-Pr₂NEt (10.4 mL, 59.8 mmol) and 2-chloro-5-nitropyrimidin-4-yl thiocyanate **10** (9.49 g, 43.8 mmol) at 10 °C. The mixture was stirred at room temperature for 30 min. The mixture was partitioned between EtOAc (150 mL) and aqueous NaHCO₃ solution (200 mL). The aqueous layer was extracted with EtOAc (2 × 30 mL). The combined organic layer was washed with brine (20 mL), dried over anhydrous Na₂SO₄ and concentrated in vacuo to give *tert*-butyl {4-methyl-3-[(5-nitro-4-thiocyanatopyrimidin-2-yl)amino]phenyl}carbamate **11** as gray solid.

To a mixture of **11** and reduced iron (6.68 g, 120 mmol) in EtOH (120 mL) and NMP (80 mL) was added a solution of calcium chloride (13.3 g, 120 mmol) in water (20 mL). The mixture was stirred at 100 °C for 16 h. It was cooled, and passed through a pad of Celite. The insoluble was washed with EtOAc (200 mL). The filtrate and washings were combined and evaporated. The residue was partitioned between EtOAc (200 mL) and water (350 mL). The aqueous layer was extracted with EtOAc (2 × 80 mL). The combined organic layer was washed with brine (50 mL) and passed through a pad of silica gel (50 g). The filtrate was concentrated to give **12** (5.24 g, 35% in three steps) as gray solid; mp 212–213 °C. ¹H NMR (300 MHz, DMSO-*d*₆) δ 1.46 (9H, s), 2.11 (3H, s), 7.04 (1H, d, *J* = 7.8 Hz), 7.14 (1H, d, *J* = 7.8 Hz), 7.43–7.77 (3H, m), 8.26 (1H, s), 8.48 (1H, br s), 9.20 (1H, br s).

5.15. *N*-[5-[(5-Amino-2-methylphenyl)amino][1,3]thiazolo[5,4-*d*]pyrimidin-2-yl]acetamide (13)

To a solution of **12** (1.20 g, 3.22 mmol) in pyridine (20 mL) was added acetyl chloride at 0 °C. The mixture was stirred at room

temperature for 1 h. It was then partitioned between EtOAc (50 mL) and aqueous NaHCO₃ solution (50 mL). The aqueous layer was extracted with EtOAc (10 mL). The combined organic layer was washed with brine (10 mL), and passed through a pad of basic silica gel (10 g). The filtrate was concentrated and recrystallized from EtOAc to give *tert*-butyl (3-[[2-(acetylamino)[1,3]thiazolo[5,4-*d*]pyrimidin-5-yl]amino]-4-methylphenyl) carbamate (1.31 g, 98%) as pale purple solid; mp 218–219 °C. ¹H NMR (300 MHz, DMSO-*d*₆) δ 1.46 (9H, s), 2.12 (3H, s), 2.18 (3H, s), 7.07 (1H, d, *J* = 8.4 Hz), 7.18 (1H, dd, *J* = 8.4, 2.1 Hz), 7.60 (1H, d, *J* = 2.1 Hz), 8.71 (1H, s), 8.88 (1H, br s), 9.23 (1H, br s), 12.33 (1H, br s).

A mixture of *tert*-butyl (3-[[2-(acetylamino)[1,3]thiazolo[5,4-*d*]pyrimidin-5-yl]amino]-4-methylphenyl) carbamate (1.27 g) and anisole (2 mL) in TFA (20 mL) was stirred at 0 °C for 1 h. It was then concentrated, and the residue was partitioned a mixed solvent of EtOAc/THF (1:1, 50 mL) and aqueous NaHCO₃ solution (50 mL). The aqueous layer was extracted with a mixed solvent of EtOAc/THF (1:1, 2 × 10 mL). The combined organic layer was washed with brine (5 mL), dried over anhydrous Na₂SO₄ and concentrated in vacuo to give **13** (795 mg, 83%) as purple solid; mp 257–258 °C. ¹H NMR (300 MHz, DMSO-*d*₆) δ 2.03 (3H, s), 2.18 (3H, s), 4.83 (2H, br s), 6.31 (1H, dd, *J* = 8.2, 2.4 Hz), 6.76 (1H, d, *J* = 2.4 Hz), 6.84 (1H, d, *J* = 8.2 Hz), 8.67 (1H, br s), 8.70 (1H, s), 12.31 (1H, br s).

5.16. Methyl 3-(2-cyanoethyl)benzoate (15)

To a suspension of methyl 2-formylbenzoate **14** (2.00 g, 12.2 mmol) and K₂CO₃ (2.02 g, 14.6 mmol) in THF (20 mL)/water (0.4 mL) was added diethyl (cyanomethyl)phosphonate (2.29 mL, 14.6 mmol). The reaction mixture was stirred at 60 °C for 1 h, and then partitioned between EtOAc (50 mL) and water (50 mL). The separated aqueous layer was extracted with EtOAc (20 mL). The combined organic layers were washed with brine (10 mL), dried over Na₂SO₄ and concentrated under reduced pressure to give methyl 3-(2-cyanoethyl)benzoate as colorless solid (ca. 5:1 *E/Z* mixture). This material was used for the next reaction without further purification.

A mixture of methyl 3-(2-cyanoethyl)benzoate and 10% Pd/C (648 mg, 0.609 mmol, 648 mg) in EtOH/THF (3:1, 60 mL) was stirred at room temperature under H₂ atmosphere (1 atm) for 2 h. The mixture was passed through Celite pad and the filtrate was concentrated under reduced pressure. The residue was purified by silica gel chromatography (30 g, 10–25% EtOAc in *n*-hexane) to give compound **15** as colorless oil (2.03 g, 88% in two steps). ¹H NMR (300 MHz, DMSO-*d*₆) δ 2.85 (2H, dt, *J* = 6.9, 1.2 Hz), 2.93–3.00 (2H, m), 3.86 (3H, s), 7.49 (1H, t, *J* = 7.6 Hz), 7.60 (1H, dt, *J* = 7.6, 1.5 Hz), 7.86 (1H, dt, *J* = 7.6, 1.5 Hz), 7.91 (1H, t, *J* = 1.5 Hz).

5.17. Methyl 3-(2-cyano-2-methylpropyl)benzoate (16)

To a solution of methyl 3-(2-cyanoethyl)benzoate **15** (510 mg, 2.70 mmol) and iodomethane (0.671 mL, 10.8 mmol) in THF (15 mL) was added dropwise a solution of LHMDS (1.1 M in THF, 7.35 mL, 8.09 mmol) in THF (10 mL) at –78 °C over 30 min. The mixture was stirred at –78 °C for 1 h, and then poured into a mixture of EtOAc (50 mL) and aqueous NH₄Cl (50 mL). The mixture was partitioned and the separated organic layer was washed with brine (10 mL), dried over anhydrous Na₂SO₄ and concentrated under reduced pressure. The residue was purified by silica gel chromatography (12 g, 5–15% EtOAc in *n*-hexane) to give **16** as yellow oil (260 mg, 44%). ¹H NMR (300 MHz, DMSO-*d*₆) δ 1.30 (6H, s), 2.94 (2H, s), 3.86 (3H, s), 7.52 (1H, t, *J* = 7.8 Hz), 7.58 (1H, dt, *J* = 7.8, 1.6 Hz), 7.87–7.93 (2H, m).

5.18. 3-(2-Cyanoethyl)benzoic acid (17a)

To a solution of **15** (169 mg, 0.893 mmol) in MeOH/THF (3:1, 4 mL) was added 2 N NaOH (0.893 mL, 1.79 mmol). The reaction mixture was stirred at 60 °C for 4 h, and then acidified with 6 N hydrochloric acid (0.5 mL). The mixture was partitioned between EtOAc (20 mL) and 1 N hydrochloric acid (15 mL). The separated aqueous layer was extracted with EtOAc (5 mL). The combined organic layers were washed with brine (5 mL), dried over anhydrous Na₂SO₄ and concentrated under reduced pressure to give compound **17a** (151 mg, 96%) as colorless crystals; mp 153–154 °C. ¹H NMR (300 MHz, DMSO-*d*₆) δ 2.80–2.89 (2H, m), 2.91–3.00 (2H, m), 7.46 (1H, t, *J* = 7.6 Hz), 7.56 (1H, dt, *J* = 7.6, 1.5 Hz), 7.83 (1H, dt, *J* = 7.6, 1.5 Hz), 7.89 (1H, t, *J* = 1.5 Hz), 12.94 (1H, br s).

5.19. 3-(2-Cyano-2-methylpropyl)benzoic acid (17b)

Compound **17b** (230 mg) was prepared from **16** (260 mg, 1.20 mmol) and 2 N NaOH (1.20 mL, 2.39 mmol) by the method similar to that described for **17a**. Yield: 95%; colorless crystals; crystallized from EtOAc; mp 144–145 °C. ¹H NMR (300 MHz, DMSO-*d*₆) δ 1.31 (6H, s), 2.93 (2H, s), 7.43–7.58 (2H, m), 7.81–7.92 (2H, m), 12.98 (1H, br s).

5.20. Methyl 3-(cyanomethoxy)benzoate (19a)

To a suspension of methyl 2-hydroxybenzoate **18a** (5.00 g, 32.9 mmol) and K₂CO₃ (6.81 g, 49.3 mmol) in acetone (60 mL) was added bromoacetonitrile (2.63 mL, 39.4 mmol). The reaction mixture was stirred at 60 °C for 4 h, and then partitioned between EtOAc (100 mL) and aqueous NaHCO₃ (100 mL). The separated aqueous layer was extracted with EtOAc (30 mL). The combined organic layers were washed with brine (10 mL), dried over anhydrous MgSO₄ and concentrated under reduced pressure. The residue was purified by basic silica gel chromatography (100 g, 10–20% EtOAc in *n*-hexane) to give compound **19a** as colorless solid (5.43 g, 86%). ¹H NMR (300 MHz, DMSO-*d*₆) δ 3.87 (3H, s), 5.27 (2H, s), 7.37 (1H, ddd, *J* = 8.1, 2.6, 1.3 Hz), 7.54 (1H, t, *J* = 8.1 Hz), 7.59 (1H, dd, *J* = 2.6, 1.3 Hz), 7.68 (1H, dt, *J* = 8.1, 1.3 Hz).

5.21. Methyl 2-chloro-3-(cyanomethoxy)benzoate (19b)

Compound **19b** (57.8 g) was prepared from methyl 2-chloro-3-hydroxybenzoate **18b** (52.0 g, 279 mmol), K₂CO₃ (57.9 g, 419 mmol), sodium iodide (62.8 g, 419 mmol), and chloroacetonitrile (19.5 mL, 307 mmol) by the method similar to that described for **19a**. Yield: 92%; colorless amorphous solid. ¹H NMR (300 MHz, DMSO-*d*₆) δ 3.87 (3H, s), 5.34 (2H, s), 7.43–7.52 (3H, m).

5.22. Methyl 3-(1-cyano-1-methylethoxy)benzoate (20a)

Compound **20a** (2.07 g) was prepared from **19a** (6.00 g, 31.4 mmol), iodomethane (15.6 mL, 251 mmol) and LHMDs (1.1 M in THF, 62.8 mL, 69.0 mmol) by the method similar to that described for **17**. Yield: 30%; yellow oil. ¹H NMR (300 MHz, DMSO-*d*₆) δ 1.72 (6H, s), 3.87 (3H, s), 7.47 (1H, ddd, *J* = 8.0, 2.4, 1.2 Hz), 7.58 (1H, t, *J* = 8.0 Hz), 7.71–7.74 (1H, m), 7.80 (1H, dt, *J* = 8.0, 1.2 Hz).

5.23. Methyl 2-chloro-3-(1-cyano-1-methylethoxy)benzoate (20b)

To a solution of **19b** (15.2 g, 67.4 mmol) and iodomethane (12.6 mL, 202 mmol) in THF (200 mL) was added dropwise a solution of NaHMDS (1.9 M in THF, 78.0 mL, 148 mmol) in THF (50 mL)

at 0 °C over 1 h. The reaction mixture was stirred at room temperature for 30 min, and then poured into a mixture of EtOAc (150 mL) and aqueous NH₄Cl (150 mL). The separated aqueous layer was extracted with EtOAc (50 mL). The combined organic layers were washed with brine (30 mL), dried over MgSO₄ and concentrated under reduced pressure. The residue was dissolved in EtOAc (100 mL) and passed through a pad of silica gel (100 g, EtOAc: 250 mL). The filtrate was concentrated under reduced pressure and the residue was purified by basic silica gel column chromatography (400 g, 0–15% EtOAc in *n*-hexane) to give **20b** as pale yellow oil (8.55 g, 50%). ¹H NMR (300 MHz, DMSO-*d*₆) δ 1.70 (6H, s), 3.80 (3H, s), 7.44 (1H, t, *J* = 7.9 Hz), 7.51 (1H, dd, *J* = 7.9, 1.8 Hz), 7.59 (1H, dd, *J* = 7.9, 1.8 Hz).

5.24. 3-(1-Cyano-1-methylethoxy)benzoic acid (21a)

Compound **21a** (1.01 g) was prepared from **20a** (2.07 g, 9.44 mmol) and 2 N NaOH (9.44 mL, 18.9 mmol) by the method similar to that described for **17a**. Yield, 51%, colorless crystals; crystallized from EtOAc/*n*-hexane; mp 93–94 °C. ¹H NMR (300 MHz, DMSO-*d*₆) δ 1.71 (6H, s), 7.42 (1H, ddd, *J* = 8.0, 2.4, 1.2 Hz), 7.53 (1H, t, *J* = 8.0 Hz), 7.69–7.73 (1H, m), 7.77 (1H, dt, *J* = 8.0, 1.2 Hz), 13.10 (1H, br s).

5.25. 2-Chloro-3-(1-cyano-1-methylethoxy)benzoic acid (21b)

To a solution of **20b** (19.0 g, 74.7 mmol) in *i*-PrOH (250 mL) was added 2 N aqueous NaOH (44.8 mL, 89.7 mmol). The reaction mixture was stirred at room temperature for 2 h, and then concentrated under reduced pressure. The residue was dissolved in EtOAc/water (5:1, 360 mL) and acidified with 1 N hydrochloric acid (90 mL). The separated aqueous layer was extracted with EtOAc (50 mL). The combined organic layers were washed with brine (30 mL), dried over anhydrous MgSO₄ and concentrated under reduced pressure. The residue was crystallized with EtOH/water (35 mL/60 mL) to give **21b** (13.9 g, 77%) as colorless crystals; mp 131–133 °C. ¹H NMR (300 MHz, DMSO-*d*₆) δ 1.77 (6H, s), 7.47 (1H, t, *J* = 7.9 Hz), 7.55 (1H, dd, *J* = 7.9, 1.9 Hz), 7.61 (1H, dd, *J* = 7.9, 1.9 Hz), 13.55 (1H, br s).

5.26. *tert*-Butyl (5-amino-2-fluorophenyl)carbamate (23)

A mixture of 2-fluoro-5-nitroaniline **22** (28.7 g, 184 mmol) and Boc₂O (100 g, 460 mmol) was stirred at 80 °C for 24 h. After cooling, the reaction mixture was directly purified by basic silica gel column chromatography (500 g, 0–10% EtOAc in *n*-hexane) to give a mixture of *tert*-butyl (2-fluoro-5-nitrophenyl)carbamate and *di-tert*-butyl (2-fluoro-5-nitrophenyl)imidodicarbonate as yellow oil. This material was used for the next reaction without further purification.

To a solution of the crude mixture in EtOH/THF (10:1, 660 mL) was added 10% Pd/C (12.0 g, 11.2 mmol). The reaction mixture was stirred at room temperature under H₂ atmosphere (1 atm) for 24 h, then passed through a pad of Celite and concentrated under reduced pressure to give a mixture of **23** and *di-tert*-butyl (5-amino-2-fluorophenyl)imidodicarbonate.

To a solution of the crude mixture in MeOH/THF (4:1, 250 mL) was added K₂CO₃ (25.4 g, 184 mmol). The reaction mixture was stirred at 60 °C for 4 h, then passed through a pad of Celite. The filtrate was concentrated under reduced pressure and the residue was partitioned between EtOAc (300 mL) and water (200 mL). The separated aqueous layer was extracted with EtOAc (100 mL). The combined organic layers were washed with brine (100 mL), dried over anhydrous Na₂SO₄ and concentrated under reduced pressure. The residue was crystallized with EtOAc/*n*-hexane to give

23 (21 g) as beige crystals. The filtrate was concentrated under reduced pressure, and the residue was purified by basic silica gel column chromatography (200 g, 5–20% EtOAc in *n*-hexane) to give **23** (5.3 g) as yellow crystals; mp 94–95 °C. Combined yield: 63% in three steps. ¹H NMR (300 MHz, DMSO-*d*₆) δ 1.44 (9H, s), 4.90 (2H, br s), 6.23 (1H, ddd, *J* = 8.8, 4.0, 2.8 Hz), 6.80 (1H, dd, *J* = 10.9, 8.8 Hz), 6.84 (1H, dd, *J* = 6.9, 2.8 Hz), 8.57 (1H, br s). Anal. Calcd for C₁₁H₁₅FN₂O₂: C, 58.40; H, 6.68; N, 12.38. Found: C, 58.32; H, 6.73; N, 12.44.

5.27. *tert*-Butyl [2-fluoro-5-(methylamino)phenyl]carbamate (**24**)

A mixture of Ac₂O (5.01 mL, 53.0 mmol) and formic acid (8.34 mL, 221 mmol) was stirred at room temperature for 30 min. To a solution of **23** (10.0 g, 44.2 mmol) in THF (60 mL) was added the abovementioned reaction mixture at 10 °C. The resulting mixture was stirred at room temperature for 16 h. The resulting mixture was partitioned between EtOAc (100 mL) and aqueous saturated NaHCO₃ (100 mL). The separated aqueous layer was extracted with EtOAc (30 mL). The combined organic layer was washed with brine (10 mL), and then passed through a pad of silica gel (100 g) using 50% EtOAc in *n*-hexane. The filtrate was concentrated in vacuo to dryness. The resulting residue was dissolved into THF (100 mL). To the mixture was added borane–dimethyl sulfide complex (11.7 mL, 111 mmol) at room temperature. The mixture was stirred at room temperature for 1.5 h. Then, MeOH (20 mL) and AcOH (10 mL) were added. The mixture was stirred at room temperature for 30 min. The resulting mixture was concentrated in vacuo, and the residue was partitioned between EtOAc (100 mL) and aqueous NaHCO₃ (100 mL). The separated aqueous layer was extracted with EtOAc (30 mL). The combined organic layer was washed with brine (20 mL), dried over anhydrous Na₂SO₄ and concentrated in vacuo. The residue was purified with silica gel column chromatography (200 g, 0–10% EtOAc in *n*-hexane) to give **24** (7.80 g, 73%) as yellow oil. ¹H NMR (300 MHz, DMSO-*d*₆) δ 1.45 (9H, s), 2.61 (3H, d, *J* = 5.1 Hz), 5.52 (1H, q, *J* = 5.1 Hz), 6.20 (1H, ddd, *J* = 8.8, 3.7, 2.8 Hz), 6.80 (1H, dd, *J* = 6.8, 2.8 Hz), 6.89 (1H, dd, *J* = 10.7, 8.8 Hz), 8.62 (1H, br s).

5.28. *tert*-Butyl [5-[(5-aminopyridin-2-yl)(methylamino)-2-fluorophenyl]carbamate (**25**)

To a solution of **24** (2.13 g, 8.87 mmol) in DMSO (5.9 mL) was added 2-chloro-5-nitropyridine (1.69 g, 10.6 mmol). The reaction mixture was stirred at 60 °C for 19 h, and then partitioned between EtOAc (50 mL) and aqueous NaHCO₃ (50 mL). The separated aqueous layer was extracted with EtOAc (20 mL). The combined organic layers were washed with brine (10 mL), dried over anhydrous Na₂SO₄ and concentrated under reduced pressure. The residue was purified by basic silica gel column chromatography (100 g, 5–15% EtOAc in *n*-hexane) to give *tert*-butyl [2-fluoro-5-[methyl(5-nitropyridin-2-yl)amino]phenyl]carbamate (1.35 g, 42%) as yellow amorphous solid. ¹H NMR (300 MHz, DMSO-*d*₆) δ 1.45 (9H, s), 3.48 (3H, s), 6.43 (1H, d, *J* = 9.5 Hz), 7.12 (1H, ddd, *J* = 8.8, 4.2, 2.6 Hz), 7.36 (1H, dd, *J* = 10.7, 8.8 Hz), 7.69 (1H, dd, *J* = 7.1, 2.6 Hz), 8.17 (1H, dd, *J* = 9.5, 2.7 Hz), 9.04 (1H, d, *J* = 2.7 Hz), 9.22 (1H, br s).

Compound **25** (1.08 g) was prepared from *tert*-butyl [2-fluoro-5-[methyl(5-nitropyridin-2-yl)amino]phenyl]carbamate (1.35 g, 3.73 mmol) and 10% Pd/C (198 mg) by the method similar to that described for **10**. Yield: 87%; purple amorphous solid. ¹H NMR (300 MHz, DMSO-*d*₆) δ 1.43 (9H, s), 3.21 (3H, s), 4.81 (2H, br s), 6.58 (1H, dd, *J* = 8.7, 0.6 Hz), 6.73 (1H, ddd, *J* = 8.9, 4.1, 2.8 Hz), 6.88 (1H, dd, *J* = 8.7, 2.8 Hz), 7.08 (1H, dd, *J* = 10.6, 8.9 Hz), 7.28 (1H, dd, *J* = 7.1, 2.8 Hz), 7.66 (1H, dd, *J* = 2.8, 0.6 Hz), 8.87 (1H, br s).

5.29. *tert*-Butyl [5-[(2-amino[1,3]thiazolo[5,4-*b*]pyridin-5-yl)(methylamino)-2-fluorophenyl]carbamate (**26**)

To a solution of potassium thiocyanate (1.26 g, 13.0 mmol) in AcOH (30 mL) was added **25** (1.08 g, 3.25 mmol). To the resulting mixture was added dropwise a solution of bromine (545 mg, 3.41 mmol) in AcOH (5 mL) at 10 °C over 10 min, and the reaction mixture was stirred at room temperature for 1 h. Additional amount of bromine (260 mg, 1.62 mmol) was added and the mixture was stirred for 30 min, and then passed through a pad of Celite and concentrated under reduced pressure. The residue was partitioned between EtOAc/THF (1:1, 100 mL) and aqueous NaHCO₃ (50 mL). The separated aqueous layer was extracted with EtOAc (20 mL). The combined organic layers were washed with brine (10 mL), dried over anhydrous Na₂SO₄ and concentrated under reduced pressure. The residue was purified by basic silica gel column chromatography (30 g, 60–80% EtOAc in *n*-hexane) to give **26** (613 mg, 48%) as red amorphous solid. ¹H NMR (300 MHz, DMSO-*d*₆) δ 1.44 (9H, s), 3.31 (3H, s), 6.44 (1H, d, *J* = 8.8 Hz), 6.97 (1H, ddd, *J* = 8.7, 4.2, 2.6 Hz), 7.21 (1H, dd, *J* = 10.6, 8.7 Hz), 7.30 (2H, br s), 7.40 (1H, d, *J* = 8.8 Hz), 7.52 (1H, dd, *J* = 7.1, 2.6 Hz), 9.04 (1H, br s).

5.30. *N*-[5-[(3-Amino-4-fluorophenyl)(methylamino)-[1,3]thiazolo[5,4-*b*]pyridin-2-yl]acetamide (**27**)

Compound **27** (546 mg) was prepared from **26** (740 mg, 1.90 mmol), acetyl chloride (0.339 mL, 4.75 mmol), pyridine (20 mL) and TFA/anisole (20:1, 21 mL) by the method similar to that described for **13**. Yield: 86%; pale purple crystals; recrystallized from EtOAc; mp 262–266 °C. ¹H NMR (300 MHz, DMSO-*d*₆) δ 2.17 (3H, s), 3.34 (3H, s), 5.28 (2H, br s), 6.40–6.47 (1H, m), 6.50 (1H, d, *J* = 9.1 Hz), 6.67 (1H, dd, *J* = 8.4, 2.6 Hz), 7.05 (1H, dd, *J* = 11.3, 8.4 Hz), 7.72 (1H, d, *J* = 9.1 Hz), 12.12 (1H, br s). Anal. Calcd for C₁₅H₁₄FN₅OS: C, 54.37; H, 4.26; N, 21.13. Found: C, 54.47; H, 4.31; N, 20.98.

5.31. *N*-[5-[(3-Amino-4-fluorophenyl)(methylamino)-[1,3]thiazolo[5,4-*b*]pyridin-2-yl]cyclopropane carboxamide (**28**)

Compound **28** (55 mg) was prepared from **26** (80 mg, 0.21 mmol), cyclopropanecarbonyl chloride (24 μL, 0.27 mmol), pyridine (1.0 mL) and TFA/anisole (10:1, 2.2 mL) by the method similar to that described for **13**. Yield: 75%; colorless crystals; recrystallized from EtOAc; mp 240–242 °C. ¹H NMR (300 MHz, DMSO-*d*₆) δ 0.90–0.97 (4H, m), 1.90–2.05 (1H, m), 3.33 (3H, s), 5.27 (2H, br s), 6.40–6.47 (1H, m), 6.51 (1H, d, *J* = 9.0 Hz), 6.67 (1H, dd, *J* = 8.2, 2.5 Hz), 7.05 (1H, dd, *J* = 11.3, 8.6 Hz), 7.71 (1H, d, *J* = 9.0 Hz), 12.41 (1H, br s). Anal. Calcd for C₁₇H₁₆FN₅OS: C, 57.13; H, 4.51; N, 19.59. Found: C, 57.01; H, 4.45; N, 19.37.

5.32. Di-*tert*-butyl (5-amino-2-fluorophenyl)imidodicarbonate (**29**)

To a solution of 2-fluoro-5-nitroaniline **22** (15.6 g, 100 mmol) in dichloromethane (200 mL) were added di-*tert*-butyl bicarbonate (87.2 g, 400 mmol) and Et₃N (20.4 g, 200 mmol), and the mixture was stirred at 55 °C for 12 h. The reaction mixture was concentrated under reduced pressure, and the residue was purified by silica gel column chromatography (10% ethyl acetate in petroleum ether) to give di-*tert*-butyl (2-fluoro-5-nitrophenyl)imidodicarbonate (19.3 g, 72%) as yellow powder. ¹H NMR (CDCl₃) δ 1.44 (18H, s), 8.12–8.16 (1H, m), 8.21–8.25 (2H, m).

To a solution of di-*tert*-butyl (2-fluoro-5-nitrophenyl)imidodicarbonate (256 mg, 0.718 mmol) in MeOH (10 mL) was added

10% Pd/C (50 mg), and the mixture was stirred under H₂ atmosphere at room temperature for 12 h. Insoluble was filtered off by through a pad of Celite, and the filtrate was concentrated under reduced pressure to give **29** (150 mg, 64%) as colorless powder: ¹H NMR (CDCl₃) δ 1.42 (18H, s), 3.55 (2H, br s), 6.46–6.54 (1H, m), 6.55–6.59 (1H, m), 6.85–6.92 (1H, m).

5.33. *N*-(5-Chloro[1,3]thiazolo[5,4-*b*]pyridin-2-yl)cyclopropanecarboxamide (**31**)

To a solution of cyclopropanecarboxylic acid (129 mg, 1.50 mmol) in dichloromethane (5 mL) were added oxalyl chloride (190 mg, 1.50 mmol) and DMF (40 μL), and the mixture was stirred at room temperature for 1 h. The reaction mixture was added to a solution (10 mL) of commercially available **30** (185 mg, 1.00 mmol) in THF at 0 °C, and the mixture was stirred for 2 h. To the reaction mixture was added water (10 mL), and the mixture was extracted with EtOAc (3 × 30 mL). The organic layer was concentrated under reduced pressure to give **31** (76 mg, 30 %) as colorless powder; ¹H NMR (CDCl₃) δ 1.02–1.06 (2H, m), 1.23–1.30 (2H, m), 1.51–1.69 (1H, m), 7.38 (1H, d, *J* = 8.7 Hz), 7.92 (1H, d, *J* = 8.7 Hz), 9.93 (1H, br s).

5.34. *tert*-Butyl [5-({2-[(cyclopropylcarbonyl)amino][1,3]-thiazolo[5,4-*b*]pyridin-5-yl)amino)-2-fluorophenyl]carbamate (**32**)

To a mixture of **31** (76 mg, 0.30 mmol), **29** (98 mg, 0.300 mmol), tris(dibenzylideneacetone)dipalladium (57 mg, 0.06 mmol), dicyclohexyl(2',4',6'-triisopropylbiphenyl-2-yl)phosphine (X-phos) (15 mg, 0.03 mmol) and potassium *tert*-butoxide (145 mg, 1.40 mmol) was added *tert*-butanol (20 mL) under nitrogen atmosphere, and the mixture was stirred under a microwave irradiation at 90 °C for 35 min. To the reaction mixture was added water (5 mL), and the mixture was extracted with ethyl acetate (3 × 50 mL). The organic layer was dried over anhydrous sodium sulfate, and concentrated under reduced pressure. The residue was purified by silica gel column chromatography (50% EtOAc in petroleum ether) to give **32** (84 mg, 63%) as brown powder. ¹H NMR (CDCl₃) δ 0.93–1.00 (2H, m), 1.25–1.28 (2H, m), 1.50 (9H, s), 1.54–1.69 (1H, m), 6.80–6.85 (3H, m), 6.97–7.05 (1H, m), 7.16–7.22 (1H, m), 7.77 (1H, d, *J* = 8.7 Hz), 8.02 (1H, dd, *J* = 7.2, 2.4 Hz), 11.56 (1H, br s).

5.35. *N*-{5-[(3-Amino-4-fluorophenyl)amino][1,3]thiazolo[5,4-*b*]pyridin-2-yl)cyclopropanecarboxamide (**33**)

To a solution of 4 N hydrogen chloride in ethyl acetate (50 mL) was added **32** (3.40 g, 7.67 mmol), and the mixture was stirred at 0 °C for 12 h. The reaction mixture was neutralized with saturated aqueous NaHCO₃, and extracted with EtOAc (3 × 50 mL). The organic layer was concentrated under reduced pressure to give **33** (1.70 g, 65%) as purple powder. ¹H NMR (DMSO-*d*₆) δ 0.92–0.97 (4H, m), 1.96–2.00 (1H, m), 5.08 (2H, br s), 6.73–6.78 (1H, m), 6.85–6.92 (2H, m), 7.16 (1H, dd, *J* = 8.4, 2.4 Hz), 7.84 (1H, d, *J* = 9.0 Hz), 8.97 (1H, s), 12.41 (1H, s).

5.36. Expression, purification, crystallization and structure determination

The kinase domain of human BRAF (residues 445–726) and human p50Cdc37 were cloned into the dual expression vector pFast-Bac Dual (Invitrogen, Life Technologies, Inc.). The encoded BRAF contained an N-terminal purification tag followed by a recombinant Tobacco Etch Virus (rTEV) protease cleavage site. The protein

was expressed in Sf9 insect cells (Invitrogen, Life Technologies, Inc.) and purified by immobilized metal-chelate affinity chromatography (IMAC). Protein bound to the IMAC column was eluted using a buffer containing 250 mM imidazole. The tag was removed by cleavage with rTEV protease in 40 mM imidazole, followed by a reverse IMAC purification. Flow through fractions containing the target protein were pooled and the protein was concentrated to a final concentration of 2.6 mg/mL in a delivery buffer of 25 mM bis-trispropane pH7.0, 250 mM NaCl, 40 mM Imidazole, 1 mM TCEP, 25% Glycerol. 1 mM of **5** was added to the protein to grow macro seed crystals or diffraction quality crystals, respectively. Small macro seed crystals were washed with well solution and transferred by hand to a fresh drop containing 1 μL well solution + 1 μL B-RAF protein in delivery buffer + 1 mM compound **5**. The crystallization condition for the macro seed crystals was 14 % PEG 8000, 0.8 M Lithium Cl, 0.06 M Tris_base and 0.04 M Tris Cl, while the crystallization conditions to support growth of the macro seeds was 7.8 % PEG 8000, 0.8 M Lithium Cl, 0.07 M Tris_base and 0.03 M Tris Cl. Crystals were harvested and frozen by flash freezing in liquid nitrogen using 25% ethylene glycol in mother liquor. The crystals diffracted to 2.95 Å with clear omit electron density for the compound. X-ray diffraction data were collected at the Advanced Photon Source (APS) beam line ID-23B, and processed using the program HKL2000.¹⁶ The structure was determined by molecular replacement using MOLREP,¹⁷ utilizing the published coordinates of B-RAF with accession code 1UWH.¹⁸ Subsequent structure refinement and model building were performed utilizing REFMAC and XtalView.^{19,20} Compound **5** was bound into the active site and clearly visible in the electron density maps. The figure was generated using PyMol Molecular Graphics System, Version 1.3 (Schrödinger, LLC).

5.37. Determination of BRAF(V600E) kinase inhibitory activity

Recombinant BRAF(V600E) protein was expressed as N-terminal FLAG-tagged protein using a baculovirus expression system. Recombinant GSTP1-MEK1 (K96R) protein was prepared using FreeStyle 293 expression system (Invitrogen Life Technologies, Carlsbad, CA). Test compounds (2.5 μL) dissolved in dimethyl sulfoxide (DMSO) were added to 37.5 μL of a reaction solution (25 mM HEPES (pH 7.5), 10 mM magnesium acetate, 1 mM dithiothreitol) containing 25 ng of BRAF(V600E) enzyme and 250 ng of recombinant protein GSTP1-MEK1 (K96R) prepared using FreeStyle 293 expression system (Invitrogen), and the mixture was incubated at room temperature for 10 min. Ten microliters of ATP solution (2.5 μM ATP, 0.1 μCi [^γ-³²P]ATP) was added to the obtained mixture, and the mixture was reacted at room temperature for 20 min. The reaction was quenched by adding 50 μL of ice-cooled 20% trichloroacetic acid (Wako Pure Chemical Industries, Ltd) to the reaction solution. The reaction solution was allowed to stand at 4 °C for 30 min, and the acid-precipitable fraction was transferred to GF/C filter plate (Millipore Corporation) using cell harvester (PerkinElmer). The plates were dried at 45 °C for 60 min, and 40 μL of MicroScinti 0 (PerkinElmer) was added thereto. The radioactivity was measured using TopCount (PerkinElmer). The kinase inhibitory rate (%) of the test compounds was calculated by the following formula:

$$\text{Inhibitory rate (\%)} = (1 - (\text{count of test compound} - \text{blank}) \div (\text{control} - \text{blank})) \times 100$$

The count of the solution reacted without addition of the compound was used as a 'control', and the count of the solution without the compound and enzyme was used as a 'blank'. The concentration of inhibitor producing 50% inhibition of the kinase

activities (IC_{50} values) and 95% confidence intervals (95% CI) for BRAF(V600E) were analyzed using GraphPad Prism version 5.01, GraphPad Software (USA).

5.38. Measurement of inhibitory activities against VEGFR2

VEGFR2 kinase activity was determined by use of an anti-phosphotyrosine antibody with quantitation performed through the AlphaScreen® system (PerkinElmer, USA). Enzyme reactions were performed in 50 mM Tris-HCl pH 7.5, 5 mM $MnCl_2$, 5 mM $MgCl_2$, 0.01% Tween-20 and 2 mM DTT, containing 10 μ M ATP, 0.1 μ g/mL biotinylated poly-GluTyr (4:1) and 0.1 nM of VEGFR2 (Millipore, UK).

Prior to catalytic initiation with ATP, compound and enzyme were incubated for 5 min at room temperature. The reactions were quenched by the addition of 25 μ L of 100 mM EDTA, 10 μ g/mL AlphaScreen streptavidine donor beads and 10 μ g/mL acceptor beads in 62.5 mM HEPES pH 7.4, 250 mM NaCl, and 0.1% BSA. Plates were incubated in the dark overnight and then read by EnVision 2102 Multilabel Reader (PerkinElmer). Wells containing the substrate and the enzyme without compound were used as total reaction control. Wells containing biotinylated poly-GluTyr (4:1) and enzyme without ATP were used as basal control. The concentration of inhibitor producing 50% inhibition of the kinase activities (IC_{50} values) and 95% confidence intervals (95% CI) for VEGFR2 were analyzed using GraphPad Prism version 5.01, GraphPad Software (USA). Sigmoidal dose–response (variable slope) curves were fitted using non-linear regression analysis, with the top and bottom of the curve constrained at 100 and 0, respectively.

5.39. Cell proliferation assay

HT29 cells were seeded into a 96-well plate at 3000 cells/well and were incubated overnight at 37 °C in a 5% CO_2 incubator. Various concentrations of the test compounds were added, and the cells were cultured for a further 3 days. Cell viability was assessed by relative cellular ATP levels using CellTiter-Glo luminescent cell viability assay (Promega) according to the manufacturer's instruction. The IC_{50} values and 95% confidence intervals (95% CI) were calculated from a dose–response curve generated by least-squares linear regression of the response.

For HUVECs, cells (3×10^3 cells/well) were seeded into 96-well plates and cultured overnight. Compounds were added to the plates with VEGF (final concentration: 60 ng/mL) and the cells were cultured for 5 days. Cellular proliferation was assessed by adding Cell Counting Kit-8 reagent (10 μ L/well; DOJINDO Laboratories, Kumamoto, Japan), incubation for several hours, and measurement of the absorbance at 450 nm with a microplate reader (BioRad Labs, Hercules, CA). The concentration causing 50% inhibition (IC_{50}) was calculated from the dose–response curve generated by least-squares linear regression analysis of the response using SAS software and the NLIN procedure (version 5.0; SAS Institute Japan, Inc., Tokyo, Japan).

5.40. In vivo pharmacodynamic (PD) study

At 10 days after transplantation, compound **5c** was suspended in 0.5% methyl cellulose solution in distilled water, and the resulting suspension was orally administered to nude rats having an engrafted tumor with a tumor volume of 300–600 mm^3 . After 4 h after administration of **5c**, the tumor was collected under ether anesthesia and the tumor was homogenized in radio-immunoprecipitation assay (RIPA) buffer (1% NP-40, 0.5% sodium deoxycholate, 1% SDS, 97.5% Dulbecco's phosphate buffered saline (DPBS) (GIBCO) with Protease Inhibitor Cocktail Set 3 (Calbiochem) and Phosphatase Inhibitor Cocktail 2 (Sigma)). The protein concentration in the

tumor lysate was determined by bicinchoninic acid (BCA) protein assay kit (Thermo), and adjusted to 1.25 μ g/ μ L. An equal volume of SDS sample buffer (BioRad) was added to the above-mentioned protein solution and incubated at 95 °C for 5 min. Western blotting was carried out in a manner similar to 'intracellular MEK/ERK phosphorylation inhibitory activity'.

5.41. Antitumor efficacy study

Treatments started after 1–3 weeks from inoculation when the estimated tumor mass was 300–500 mm^3 . Compound **5c** was suspended in 0.5% methyl cellulose solution in distilled water, and the resulting suspension was orally administered to nude rats. All animals were treated with vehicle (diluted water) or **5c** suspension once a day for 14 consecutive days by oral gavages. Tumor volumes were calculated as volume = $L \times l^2 \times 1/2$, where L was taken to be the longest diameter across the tumor and l was taken to be the corresponding perpendicular. Treatment over control (T/C, %), an index of antitumor efficacy, was calculated by comparison of the mean change in tumor volume over the treatment period for the control and treated groups. Body weight was also measured on the day of tumor volume assessment.

5.42. Microsome stability

In vitro oxidative metabolic studies of compounds were carried out using hepatic microsomes obtained from humans. Briefly, the incubation mixtures were prepared under ice-cold conditions by adding 50 μ L of potassium phosphate buffer (50 mmol/L, pH 7.4), 38 μ L of ultrapure water, 1 μ L of the microsomes (0.2 mg protein/mL), and 1 μ L of the compound solution (1 μ mol/L) in an eppendorf tube at the final concentrations indicated. The reactions were initiated by adding 10 μ L of the NADPH-generating system (final concentrations of 5 mmol/L $MgCl_2$, 5 mmol/L glucose 6-phosphate, 0.5 mmol/L β -NADP⁺, and 1.5 units/mL glucose-6-phosphate dehydrogenase) to the incubation mixtures. For the samples without NADPH, ultrapure water was substituted for the NADPH-generating system. Incubations were conducted at 37 °C for 20 min in a final volume of 100 μ L and terminated by adding 100 μ L of ice-cold acetonitrile. For each species, zero-time incubations which served as the controls were terminated by adding 100 μ L of ice-cold acetonitrile before adding 1 μ L of the compound solution. The samples were mixed by vortex mixing vigorously and centrifuging at 3000 \times g for 10 min at 4 °C. The supernatant fractions were subjected to high performance liquid chromatography (HPLC) with an UV detector. All incubations were made in duplicate.

5.43. Thermodynamic solubility

About 0.5 mg of sample was added to 0.5 mL of a dissolving solvents, which was 20 mmol/L bile acid in the JP 2nd fluid for disintegration solution (pH 6.8),¹⁵ and the sample solution were shaken at 37 °C for 18 h. The solution was filtered through a membrane filter (0.45 μ m). The filtrate was diluted with acetonitrile and analyzed by high-performance liquid chromatography (HPLC). The sample solutions were analyzed with an HPLC system (W2695, Waters, Milford, MA, USA) and UV detector (W2487, Waters) operated at 230 nm. The packaged column was Shiseido MG-III ODS (3 μ m, 4.6 mm \times 75 mm, Shiseido, Tokyo, Japan) operated at 40 °C at a flow rate of 1.0 mL/min. The two mobile phases used were (A) 50 mmol/mL ammonium acetate buffer and (B) acetonitrile. The elution program started at 100:0 = A:B, ramped linearly to 0:100 = A:B at 5 min, held there until 7 min, and returned to 100:0 = A:B at 8 min.

5.44. Pharmacokinetic studies

For oral cassette dosing PK study, test compounds were dissolved in a mixture of DMSO and 1,3-butylene glycol and were administered orally to non-fasted mice at a dose of 10 mg/kg. For single dosing PK study of **5c**, the compound was dissolved in a mixture of dimethylacetamide and 1,3-butanediol (1:1, v/v) and was administered intravenously to non-fasted rats at a dose of 1 mg/kg. Compound **5c** was suspended in 0.5% methylcellulose solution for oral administration and was administered orally to non-fasted rats at a dose of 25 mg/kg.

Blood samples were taken from the femoral vein at the designated time points after dosing, and centrifuged to obtain the plasma fractions. The plasma samples were de-proteinized with acetonitrile containing an internal standard. After centrifugation, the supernatant was diluted with a mixture of 0.01 mol/L ammonium formate solution and acetonitrile (9:1, v/v) and centrifuged again. The compound concentrations in the supernatant were measured by LC/MS/MS.

5.45. Calculation of stable conformation

Local energy minimum conformations of compounds in Figures 2 and 4 were calculated with molecular mechanic analysis in MOE (version 2006.0804 and 2009.1002, respectively). During the minimization procedure, the following conditions were adopted. The MMFF94s force field²¹ was set for the molecular mechanic calculation. The dielectric constant was set to $4 \times r$, where r is the interatomic distance. Atomic charges of the compounds were assigned by using the AM1-BCC method.

Acknowledgements

The authors thank Shuhei Yao, Noriko Uchiyama, Hiroshi Miki, Taeko Yoshida, and Hidehisa Iwata for their assistance in evaluating the kinase inhibitory activities. The authors also thank Kazuyo Kakoi, Juran Kato and Kenichi Iwai for their assistance in evaluating the cellular pMEK inhibitory activities, and Akira Hori and Yuichi Kakoi for their assistance in evaluating the cellular VEGFR2 inhibitory activities. The authors are grateful to Garret Textor, Matt Kroeger, and Gyorgy Snell from Takeda California for their assistance in determining the crystal structure of BRAF with **5**. The authors acknowledge the Advanced Photon Source, an Office of Science User Facility operated for the U.S. Department of Energy

(DOE) Office of Science by Argonne National Laboratory, supported by the U.S. DOE under Contract No. DE-AC02-06CH11357. Finally, the authors express their gratitude to Yukiko Watanabe for her assistance in PK evaluation.

Supplementary data

Supplementary data associated with this article can be found, in the online version, at <http://dx.doi.org/10.1016/j.bmc.2012.07.032>. These data include MOL files and InChiKeys of the most important compounds described in this article.

References and notes

- Robinson, M. J.; Cobb, M. H. *Curr. Opin. Cell Biol.* **1997**, *9*, 180.
- Roberts, P. J.; Der, C. J. *Oncogene* **2007**, *26*, 3291.
- Holmes, K.; Roberts, O. L.; Thomas, A. M.; Cross, M. J. *Cell Signal.* **2007**, *19*, 2003.
- Lang, S. A.; Schachtschneider, P.; Moser, C.; Mori, A.; Hackl, C.; Gaumann, A.; Batt, D.; Schlitt, H. J.; Geissler, E. K.; Stoeltzing, O. *Mol. Cancer Ther.* **2008**, *7*, 3509.
- Okaniwa, M.; Hirose, M.; Imada, T.; Ohashi, T.; Hayashi, Y.; Miyazaki, T.; Arita, T.; Yabuki, M.; Kakoi, K.; Kato, J.; Takagi, T.; Kawamoto, T.; Yao, S.; Sumita, A.; Tsutsumi, S.; Tottori, T.; Oki, H.; Sang, B.-C.; Yano, J.; Aertgeerts, K.; Yoshida, S.; Ishikawa, T. *J. Med. Chem.* **2012**, *55*, 3452.
- Okaniwa, M.; Imada, T.; Ohashi, T.; Miyazaki, T.; Arita, T.; Yabuki, M.; Sumita, A.; Tsutsumi, S.; Higashikawa, K.; Takagi, T.; Kawamoto, T.; Inui, Y.; Yoshida, S.; Ishikawa, T. *Bioorg. Med. Chem.* **2012**, *20*, 4680.
- Ishikawa, M.; Hashimoto, Y. *J. Med. Chem.* **2011**, *54*, 1539.
- Wenglowsky, S.; Moreno, D.; Rudolph, J.; Ran, Y.; Ahrendt, K. A. *Bioorg. Med. Chem. Lett.* **2012**, *22*, 912.
- Leach, A. G.; Jones, H. D.; Cosgrove, D. A.; Kenny, P. W.; Ruston, L.; MacFaul, P.; Wood, J. M.; Colclough, N.; Law, B. *J. Med. Chem.* **2006**, *49*, 6672.
- Fujita, Y.; Yonehara, M.; Tetsuhashi, M.; Noguchi-Yachide, T.; Hashimoto, Y.; Ishikawa, M. *Bioorg. Med. Chem.* **2010**, *18*, 1194.
- Naito, T.; Inoue, S. *Chem. Pharm. Bull.* **1958**, *6*, 338.
- Wadsworth, W. S.; Emmons, W. D. *J. Am. Chem. Soc.* **1961**, *83*, 1733.
- Huang, X.; Anderson, K. W.; Zim, D.; Jiang, L.; Klapars, A.; Buchwald, S. L. *J. Am. Chem. Soc.* **2003**, *125*, 6653.
- The coordinates and structure factors have been deposited with the Protein Data Bank with accession code 4FCO.
- The Ministry of Health, Labour and Welfare Ministerial Notification No. 285, <http://jpub.nihs.go.jp/jp15e/>, General tests/reagents, test solutions. *The Japanese pharmacopoeia English version*, **2006**, *15*, p 239.
- Otwinowski, Z.; Minor, W. *Methods Enzymol.* **1997**, *276*, 307.
- Vagin, A.; Teplyakov, A. *J. Appl. Crystallogr.* **1997**, *30*, 1022.
- Wan, P. T. C.; Garnett, M. J.; Roe, S. M.; Lee, S.; Niculescu-Duvaz, D.; Good, V. M.; Cancer Genome Project; Jones, C. M.; Marshall, C. J.; Springer, C. J.; Barford, D.; Marais, R. *Cell* **2004**, *116*, 855–867.
- Collaborative Computational Project, Number 4. *Acta Crystallogr. D Biol. Crystallogr.* **1994**, *50*, 760.
- McRee, D. E. *J. Struct. Biol.* **1999**, *125*, 156.
- Halgren, T. A. *J. Comput. Chem.* **1999**, *20*, 720.